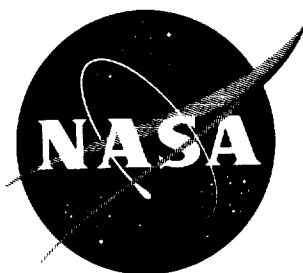


49p. N62-15422

NASA TN D-1397

NASA TN D-1397



2

TECHNICAL NOTE

D-1397

LOW-SPEED LONGITUDINAL CHARACTERISTICS OF AN
AIRPLANE CONFIGURATION INCLUDING EFFECTS OF CANARD AND
WING TRAILING-EDGE FLAP CONTROLS IN COMBINATION

By Bernard Spencer, Jr., and William C. Sleeman, Jr.

Langley Research Center
Langley Station, Hampton, Va.

NATIONAL AERONAUTICS AND SPACE ADMINISTRATION
WASHINGTON

September 1962

A

NATIONAL AERONAUTICS AND SPACE ADMINISTRATION

TECHNICAL NOTE D-1397

LOW-SPEED LONGITUDINAL CHARACTERISTICS OF AN
AIRPLANE CONFIGURATION INCLUDING EFFECTS OF CANARD AND
WING TRAILING-EDGE FLAP CONTROLS IN COMBINATION¹

By Bernard Spencer, Jr., and William C. Sleeman, Jr.

SUMMARY

An investigation of the static longitudinal stability and control characteristics of a canard-airplane configuration at low speed has been conducted in the Langley 300-MPH 7- by 10-foot tunnel. The planform of the canard control was identical to that of the wing, which had an aspect ratio of 3, a taper ratio of 0.14, and an unswept 80-percent-chord line. Effects of canard-surface size and longitudinal and vertical position were studied for the model, with only the canard surface for control. Supplementary trim or control was studied by use of wing trailing-edge flaps and by addition of an auxiliary horizontal tail behind the wing.

All the canard controls investigated were greatly limited in providing trim at high lift as a result of stalling of the canard surface at relatively low angles of attack and control deflections. The use of deflected wing trailing-edge flaps in combination with the canard control provided increases in trimmed lift coefficient over those obtained by deflection of the canard surface alone. However, these increases were achieved only with negative deflections of the trailing-edge flap, resulting in an increase in the angle of attack corresponding to a given trimmed lift coefficient. Addition of an auxiliary horizontal tail located behind and below the wing provided similar gains in maximum trimmed lift coefficient and greatly reduced the longitudinal instability encountered at high angles of attack on the basic model with the canard control.

The highest trends in canard-surface lift efficiency occurred with the small canard surface located above the fuselage center line, inasmuch as this location for the canard surface tended to minimize losses in wing lift resulting from the canard-surface wake.

¹Supersedes NASA Memorandum 4-22-59L by Bernard Spencer, Jr., and William C. Sleeman, Jr., 1959.

INTRODUCTION

Investigations conducted by the National Aeronautics and Space Administration on the use of airplane arrangements having canard controls have provided pertinent information relative to the major advantages and disadvantages to be expected from this type of configuration. (For example, see refs. 1, 2, and 3.) Favorable performance characteristics at supersonic speeds and possible reductions in trim drag obtainable by use of canard controls make the use of this type of configuration attractive when compared with conventional tail-rearward or tailless airplanes.

Subsonic results of an investigation (ref. 4) on two canard-surface arrangements indicated longitudinal-control problems at moderate and high angles of attack, resulting from stalling of the canard control. One of the purposes of the present investigation was to study means of alleviating these control problems by use of supplementary trim devices which aid in reducing the required load on the canard control for trim. Various controls studied in this investigation include either a combination of canard-surface deflection and wing trailing-edge flap control or an auxiliary horizontal tail of low aspect ratio deflected to produce trimming moments at high angles of attack.

Canard wake effects on the overall wing loading also present a problem as to the best planform, aspect ratio, and wing leading-edge position relative to canard location (ref. 3) so that optimum lifting capabilities of both surfaces may be realized. Therefore, an analysis has been made of the canard efficiency, which is simply a measure of the change in wing lift resulting from the canard wake expressed in terms of the canard lift. This analysis also includes trends in configuration performance characteristics and the relationship to trends in canard efficiency.

SYMBOLS

Results of this investigation are presented with reference to the stability-axis system shown in figure 1. Pitching-moment results of this investigation are presented about different moment reference points for each of the different configurations tested. The moment reference locations used are presented in table I. The symbols used in this investigation are defined as follows:

- c chord of wing or canard surface, ft
- \bar{c} mean aerodynamic chord of wing or canard surface, ft

L
2
2
1

C_D	drag coefficient, $\frac{\text{Drag}}{qS_w}$
C_L	lift coefficient, $\frac{\text{Lift}}{qS_w}$
C_m	pitching-moment coefficient, $\frac{\text{Pitching moment}}{qS_w \bar{c}_w}$
L/D	lift-drag ratio, $\frac{C_L}{C_D}$
M	Mach number
q	dynamic pressure, lb/sq ft
S	total area of wing or canard surface including area inside of fuselage, sq ft
S_1	exposed wing area outboard of canard-surface tip, sq ft
S_2	exposed wing area inboard of canard-surface tip, sq ft
α	angle of attack, deg
δ	deflection of control surface, positive when trailing edge is down, deg
$\Delta C_{L,c}$	total increment in C_L resulting from addition of the canard surface
$\frac{\partial \epsilon}{\partial \alpha}$	rate of change of average downwash angle across complete wing span with angle of attack
η_L	canard-surface lift-efficiency factor, $\frac{(C_L)_{WFC} - (C_L)_{WF}}{(C_L)_{FC} - (C_L)_F}$

Subscripts:

c	canard surface
f	wing trailing-edge flap
h	auxiliary horizontal tail

max maximum

w wing

Configuration designations:

A afterbody

C canard surface

C ₁	small canard surface located on fuselage center line (total area, 16 percent of total wing area)	L 2 2
----------------	--	-------------

C ₂	large canard surface located on fuselage center line (total area, 25 percent of total wing area)	1
----------------	--	---

C ₃	small canard surface located 2.5 inches above fuselage center line (total area, 16 percent of total wing area)	
----------------	--	--

E forebody extension

F forebody

W wing

MODEL DESCRIPTION

Basic Model

A drawing of the basic model is presented in the lower part of figure 2(a), and the geometric characteristics of the model are summarized in table II. A photograph of the model with the small canard surface located on the fuselage center line is shown in figure 3. The wing used in this investigation had NACA 65A006 airfoil sections parallel to the plane of symmetry and was of trapezoidal planform with an aspect ratio of 3, taper ratio of 0.14, and an unswept 80-percent-chord line. The trailing-edge flaps of the wing were hinged at the unswept 80-percent-chord line, and were full exposed span flaps. The gap between the wing and the flap was sealed for all tests. The sweepback of the quarter-chord line was 28.1°. The smaller canard surface was similar in planform and airfoil section to the wing, and the total canard-surface area was 16 percent of the total wing area.

Modifications to Basic Model

The large canard surface used in this investigation had a flat-plate section similar in planform to the wing, but the profile consisted of a rounded leading edge and beveled trailing edge. The total

area of this canard surface was 25 percent of the total wing area. The canard surface tested on top of the fuselage had the same total area as the smaller canard surface, but the profile consisted of a flat plate having rounded leading edge and beveled trailing edge.

The fuselage forebody extension, shown in the top drawing of figure 2(a), was 7 inches in diameter and 9 inches in length. A detachable afterbody, shown in the same drawing, was also 7 inches in diameter and was 15 inches in length.

The geometry of the auxiliary horizontal tail shown in figure 2(a) is given in table II. This tail was located behind and below the wing.

TESTS AND CORRECTIONS

Tests

The present investigation was conducted in the Langley 300-MPH 7- by 10-foot tunnel at a dynamic pressure of approximately 28.75 pounds per square foot. The average test Reynolds number, based on the wing mean aerodynamic chord, was approximately 1.49×10^6 . The model was mounted on a single support and tested through a maximum angle-of-attack range from -2° to 28° at fixed deflections of the canard surface of 0° , 5° , 10° , and 15° , and wing trailing-edge flap control deflections of 0° , -5° , -10° , and $\pm 20^\circ$.

Corrections

Blockage corrections determined by the method of reference 5 have been applied to the dynamic pressure, and jet-boundary corrections obtained by use of reference 6 were added to the angles of attack and drag coefficients. Lift coefficients have been corrected for effects of the static-pressure difference between the inside and outside of the tunnel test section. Drag coefficients have also been corrected for a tunnel-buoyancy effect, and pitching-moment coefficients have been corrected for support-strut tares. No base-pressure corrections have been applied.

PRESENTATION OF RESULTS

Pitching-moment data presented in this paper have been transferred to various moment reference points in order that the different configurations tested have approximately $0.10\bar{c}_w$ static margin at low lift

coefficients. This method of data presentation was adopted so that control characteristics of the different canard-surface arrangements could be compared more directly than results presented about a fixed moment reference for the complete investigation.

The effects of canard-control deflection and of wing flap deflection with and without the canard surface are presented in figures 4 to 7 for the model with large and small canard controls.

Effects of canard-control deflection for the model with forebody extension are presented in figure 8 for both the small and large canard controls, and the characteristics associated with the removal of the fuselage afterbody on the configuration with the small canard surface are given in figure 9.

L
2
2
1

Effects of the auxiliary horizontal tail used in combination with the model having the basic canard control are presented in figure 10. Figures 11 and 12 present data showing effects of the component parts for some of the configurations tested.

Summary characteristics of the various configurations are presented in figures 13 and 14, which include experimental trends in canard-surface lift-efficiency factors throughout the angle-of-attack range obtained and trends in untrimmed L/D . Figure 15 presents an analysis of trends in canard-surface efficiencies for various canard-surface arrangements throughout a Mach number range from 0.60 to 2.22.

DISCUSSION

Effects of Canard Surface on Stability

Effects of the small and the large canard surfaces on longitudinal stability are shown in figures 4(a) and 6(a), respectively. The wing-body pitching-moment characteristics indicated by dashed lines were obtained from figures 5(a) and 7(a). These results show that addition of the small and the large canard surfaces reduced the low-lift stability of the wing-body configuration approximately $0.30\bar{c}_w$ and $0.47\bar{c}_w$, respectively. Pitching moments for the complete model with both the large and small canard surfaces showed an appreciable loss in longitudinal stability for angles of attack in excess of approximately 20° .

Control Effectiveness

Canard control.- Increases in trimmed lift coefficient were obtained by deflections of the small canard control (fig. 4(a)) up to 10° surface

deflections, resulting in a maximum attainable $C_{L,trim}$ of approximately 0.48. Further deflection, however, caused the canard surface to stall, which resulted in loss of effectiveness of the canard as a control for angles of attack above approximately 8° . Reductions in static margin to $0.05\bar{c}_w$ (fig. 4(b)) increased the maximum attainable trimmed lift coefficient to approximately 0.56. Since this small canard surface yielded rather low values of maximum $C_{L,trim}$, a larger surface was tested, and the results were analogous to those attained with the smaller canard surface in that control effectiveness was lost above 10° canard-surface deflection (fig. 6(a)). Maximum attainable values of trimmed lift coefficient were increased to approximately 0.63 by use of the large canard for the configuration with a $0.10\bar{c}_w$ static margin and to approximately 0.68 for the configuration with a $0.05\bar{c}_w$ static margin (fig. 6(b)).

Since the canard-control effectiveness was poor for both canard surfaces tested because of canard-surface stalling at moderate control deflections, the fuselage forebody was extended so that the required trimming moments could be obtained at a lower lift of the canard surface. Results showing effects of extending the fuselage forebody with the small canard control (fig. 8(a)) indicated that higher values of trimmed lift coefficient at moderate control deflections were attainable with a maximum $C_{L,trim}$ of 0.63 obtained. For the large canard control tested on this configuration, maximum $C_{L,trim}$ was increased to a value of 0.65 for a surface deflection of 10° . Complete loss of control effectiveness occurred, however, above 10° control deflection for both surfaces.

For the particular arrangements tested, the use of the canard surfaces was adaptable only for configurations operating at lift coefficients below approximately 0.70. Means are available for increasing the canard lifting capabilities by employing high-lift devices or boundary-layer control on the canard surface. Incorporation of these devices would be expected to provide appreciable gains in trimming ability of the canard surface in the range of angle of attack (10° to 15°) applicable to landing attitudes.

Canard control combined with wing trailing-edge flap control.— One possible approach to increasing operational lift coefficients is the use of a canard surface and wing trailing-edge flap in combination, employing one surface as a trimmer and the other as a control; the choice depends on the effectiveness of these surfaces in either capacity. The use of this combination offers possible methods of obtaining high values of trimmed lift coefficient with the flap deflected in an up position in high-speed flight. Combinations of canard and wing trailing-edge flap deflections may also permit improved landing and take-off performance.

The use of the wing trailing-edge flap in combination with the small canard control with the wing flap used as a trimming device increased the values of maximum trimmed lift coefficient to approximately 0.74 by use of negative flap deflection (fig. 4(d)). Flap deflections in excess of -10° would not be expected to provide large increases in maximum trim lift because, in providing trimming moments at high angles of attack, the flap decreases the maximum configuration lift. (See fig. 5(a).) Similar observations may be made with regard to the large canard surface in combination with the wing trailing-edge flap (figs. 6(a) to 6(d)). Maximum attainable trimmed lift coefficient was increased to approximately 0.80 for this combination, with the flap deflected -10° (fig. 6(d)).

L
2
2
1

Use of the wing trailing-edge flap as a high-lift device is illustrated in figures 4(f) and 6(f) with the small and large canard surfaces, respectively. Comparison of the lift results with the wing flap at 0° (figs. 4(a) and 6(a)) and 20° (figs. 4(f) and 6(f)) deflection indicates increments in lift coefficient of approximately 0.4 provided by the wing flap at angles of attack up to approximately 15° . The pitching-moment data indicate, however, that neither the large nor small canard surface was capable of trimming out the large diving moment caused by the trailing-edge flap ($\delta_f = 20^\circ$) even at 0° angle of attack. (See figs. 4(f) and 6(f).)

The results obtained with the small and large canard surfaces used as a trim device, with the wing trailing-edge flap used for control, are shown in figures 5(b) and 7(b), respectively. Comparison of the range of attainable trimmed lift coefficients of the fixed canard-surface deflection and flap control, with the fixed flap deflection and canard-control combination (figs. 4(a) to 4(d) and 6(a) to 6(d)) indicates that use of the canard surface as a trim device with the flap employed as a control provides a larger range of trimmed lift coefficient. This indicates that the wing flap was a more powerful control than either of the canard surfaces. However, the presence of the deflected canard surface allows values closer to the configuration $C_{L,max}$ to be obtained than does the configuration without the canard surface (figs. 5(a) and 7(a)). The increases in maximum $C_{L,trim}$ with the canard surface and wing trailing-edge flap combination were achieved with negative deflections of the trailing-edge flap, which resulted in an increase in the angle of attack corresponding to a given trimmed lift coefficient.

Afterbody effects on control.— Tests of the model with the afterbody removed and with the small canard surface (fig. 9) showed increases of maximum attainable $C_{L,trim}$ as compared with the value obtained for a similar configuration with the afterbody attached (fig. 4(a)). Increases for maximum $C_{L,trim}$ from 0.48 ($\delta_c = 10^\circ$) to 0.72 ($\delta_c = 10^\circ$) were realized with the wing trailing-edge flap at a deflection of 0° . The instability which occurred above an angle of attack of 20° was accentuated by

removal of the afterbody; however, the region of instability occurred at a lift greater than the highest lift coefficient which could be trimmed. This effect of afterbody on stability was also noted in the tests of reference 4.

Auxiliary horizontal tail.- The use of a horizontal tail at subsonic speeds for trim and control and the rotation of this horizontal tail downward to form a ventral fin for use at supersonic speeds has also been considered as a possible method of reducing the shift in aerodynamic center at supersonic speeds without causing the longitudinal instability associated with canards in the subsonic speed range. (See ref. 7.) Comparison of the basic canard-surface configuration with the configuration having a canard surface and auxiliary horizontal tail is presented as figure 10. These configurations are presented about a similar moment reference point located $0.42\bar{c}_w$ ahead of the wing $\bar{c}_w/4$ point. Maximum values of $C_{L,trim}$ for the basic small-canard-surface configuration were increased appreciably by addition of the auxiliary horizontal tail deflected -15° . The results of figure 10 also show that the instability at high angles of attack associated with the basic small canard control was greatly reduced by addition of the auxiliary horizontal tail to the model.

Canard Efficiency

The addition of a canard surface to all of the configurations tested increased or did not affect the total lift of the configurations throughout the angle-of-attack range. Corresponding reductions in drag at a given lift coefficient for the undeflected canard controls due to the reduction in angle of attack at the wing were also noted. From figures 11 and 12, the incremental additions to lift may be seen for six configurations which represent canard surfaces of two sizes in two longitudinal and vertical locations. The addition of the canard surfaces to the body alone indicated increases in lift throughout the angle-of-attack range. The addition of the canard surfaces to the wing-body combination, however, indicates less increase in lift throughout the angle-of-attack range. These increments provided by the canard control represent the amount of overall effective lift available from the canard surface at given angles of attack. A comparison of the incremental lift due to the canard surface for wing-body and body configurations indicates that the incremental lift provided by the canard surface when added to the wing-body is less than that provided by the canard when added to the body. This loss in available lift is believed to arise from a loss in lift on the wing due to the canard downwash. This loss of lift may be related to the canard-surface lift by means of an efficiency factor. This efficiency is defined as the ratio of the incremental lift associated with the addition of the canard surface to the wing-on configuration to the lift associated with the addition of the canard surface to the wing-off configuration, and may be expressed as an equation:

$$\eta_L = \frac{(\Delta C_{L,c})_{\text{wing on}}}{(\Delta C_{L,c})_{\text{wing off}}} = \frac{(C_L)_{WFC} - (C_L)_{WF}}{(C_L)_{FC} - (C_L)_F} \quad (1)$$

Efficiency factors in lift have been computed for the six configurations denoted in figures 11 and 12 and are presented in figure 13. The estimated values of η_L were determined by use of a simple relation derived from equation (1), which is as follows:

$$\eta_L = 1 - \frac{S_w}{S_c} \frac{\partial \epsilon}{\partial \alpha}$$

L
2
2
1

This relation is valid only when the planforms of wing and canard surface are similar, and the body effects are negligible. The efficiency factors in lift and pitching moment presented in figure 13 were computed for untrimmed values of C_L and for undeflected canard surfaces. This method of presentation was adopted since the purpose of presenting efficiency factors was to indicate the variations in efficiency trends for various canard arrangements. Therefore point values represented in figure 13 should not be considered indicative of absolute values to be expected from a similar configuration.

Experimental canard-surface efficiency factors in lift (fig. 13) show that the highest efficiencies could be expected from a configuration having the canard control located in a position above the fuselage center line. This possibly could result from the canard-surface wake being placed initially above the wing surface. A comparison of experimental and estimated values of η_L for configuration WFAC₁ shows good correlation in trends throughout the angle-of-attack range; however, overestimates are noted from $\alpha \approx 4^\circ$ to 20° .

Canard-Surface Performance Characteristics

Lift-drag ratios for the six configurations tested with canard surface on and two configurations with the canard surfaces off are presented in figure 14. An approach has been used in obtaining untrimmed values of L/D for the canard arrangements analogous to those applied in determining trends in configuration efficiencies in that trends in L/D were the objective of the analysis. This method was used in order to establish relationships between trends in efficiency factors and trends in L/D .

A comparison of the trends in efficiency and in L/D for the configurations tested indicates that the highest trends in untrimmed L/D occur with the configurations having the small canard surface located above the fuselage center line which is also the configuration having the highest lift-efficiency trends. From the indications of figures 13 and 14, and since the total configuration lift is a function of canard-surface efficiency, increases in efficiency may result in increased performance. For this reason, some analysis has been made of canard-surface efficiency at various Mach numbers for different canard-airplane arrangements previously tested.

The continuous curve indicated in the top graph of figure 15 represents a configuration from reference 8 with a delta wing and a delta canard surface and with a ratio of canard area to wing area of 0.12 (designated configuration 1). The effects of increasing Mach number as indicated in this figure show appreciable losses in efficiency in going from subsonic to low supersonic speeds. Increases in efficiency are noted, however, above a Mach number of 1.1 to the test limit of 2.22. The effects of configuration on the canard-surface lift efficiency at Mach number of 2.01 are indicated in this same figure. An increase in efficiency from 0.26 to 0.46 is realized when configuration 1 is compared with configuration 2 (from ref. 3) which represents a trapezoidal canard surface on a delta-wing model. The outstanding differences between the two configurations were that the second configuration had a trapezoidal canard surface and had more wing area located outboard of the canard-surface tip. Configuration 3, which had further increases in wing area outboard of the canard tip, showed a further increase in efficiency to 0.65. This last configuration had a trapezoidal wing and trapezoidal canard surface (ref. 3). Because large increases in canard-surface lift efficiencies were noted when the wing area located outboard of the canard-surface tip was increased, the graph at the bottom of figure 15 was made to show the variation of η_L with the ratio of exposed wing area outboard of the canard-surface tip S_1 to the exposed wing area inboard of the canard-surface tip S_2 . An increase in outboard- to inboard-area ratios from approximately 1.1 to 2.8 shows increases in efficiency of approximately 150 percent. An interesting point to note is that the variation of η_L with the area ratio appears to be a linear variation.

SUMMARY OF RESULTS

Results of an experimental investigation of the longitudinal stability and control characteristics of a model having canard surface and wing trailing-edge flap controls may be summarized as follows:

1. In all of the configurations investigated, stalling of the canard surface and consequent loss of the effectiveness of the canard surface as a control occurred at relatively low control deflections and model angles of attack. Stalling of the control surface greatly limited maximum trimmed lift coefficient attainable for reasonable values of longitudinal stability.

2. Values of maximum trimmed lift coefficient could be increased significantly by use of a wing trailing-edge flap control in combination with the canard control. This increase was achieved, however, only with negative deflections of the trailing-edge flap with the result that the angle of attack corresponding to a given trimmed lift coefficient also was increased.

L
2
2
1

3. The addition of the deflected auxiliary horizontal tail to the basic canard-surface configuration provided an appreciable gain in maximum trimmed lift coefficient.

4. Pitching-moment results indicated a region of static longitudinal instability above an angle of attack of approximately 20° with either of the canard surfaces on the model. Addition of the auxiliary horizontal tail greatly reduced this instability.

5. The highest values of canard lift efficiency occurred with the small canard surface located above the fuselage center line. This configuration also provided the highest untrimmed lift-drag ratio. This location of the canard surface tended to minimize losses in wing lift resulting from the canard wake.

Langley Research Center,
National Aeronautics and Space Administration,
Langley Field, Va., January 22, 1959.

REFERENCES

1. Spearman, M. Leroy, and Driver, Cornelius: Effects of Canard Surface Size on Stability and Control Characteristics of Two Canard Airplane Configurations at Mach Numbers of 1.41 and 2.01. NACA RM L57L17a, 1958.
2. Driver, Cornelius: Longitudinal and Lateral Stability and Control Characteristics of Two Canard Airplane Configurations at Mach Numbers of 1.41 and 2.01. NACA RM L56L19, 1957.
3. Driver, Cornelius: Longitudinal and Lateral Stability and Control Characteristics of Various Combinations of the Component Parts of Two Canard Airplane Configurations at Mach Numbers of 1.41 and 2.01. NASA MEMO 10-1-58L, 1958.
4. Sleeman, William C., Jr.: Investigation at High Subsonic Speeds of the Static Longitudinal and Lateral Stability Characteristics of Two Canard Airplane Configurations. NACA RM L57J08, 1957.
5. Herriot, John G.: Blockage Corrections for Three-Dimensional-Flow Closed-Throat Wind Tunnels, With Consideration of the Effect of Compressibility. NACA Rep. 995, 1950. (Supersedes NACA RM A7B28.)
6. Gillis, Clarence L., Polhamus, Edward C., and Gray, Joseph L., Jr.: Charts for Determining Jet-Boundary Corrections for Complete Models in 7- by 10-Foot Closed Rectangular Wind Tunnels. NACA WR L-123, 1945. (Formerly NACA ARR L5G31.)
7. Sleeman, William C., Jr.: Investigation at High Subsonic Speeds of the Use of Low Auxiliary Tail Surfaces Having Dihedral to Improve the Longitudinal and Directional Stability of a T-Tail Model at High Lift. NASA TN D-804, 1961. (Supersedes NACA RM L57I24.)
8. Boyd, John W., and Peterson, Victor L.: Static Stability and Control of Canard Configurations at Mach Numbers From 0.70 to 2.22 - Longitudinal Characteristics of a Triangular Wing and Canard. NACA RM A57J15, 1958.

L
2
2
1

TABLE I

MOMENT REFERENCE LOCATIONS FOR ALL CONFIGURATIONS

TESTED FOR $\partial C_m / \partial C_L = -0.10$

Configuration*	Moment reference location from $\frac{\bar{c}_w}{4}$
WFAC ₁	0.42 \bar{c}_w ahead
WFAC ₂	.59 \bar{c}_w ahead
WFAC ₃	.42 \bar{c}_w ahead
WFEAC ₁	.48 \bar{c}_w ahead
WFEAC ₂	.70 \bar{c}_w ahead
WFEAC ₃	.48 \bar{c}_w ahead
WFC ₁	.42 \bar{c}_w ahead

* For all tests with canard surface off, longitudinal data are presented about the same moment reference as the corresponding canard-surface-on moment reference.

L
2
2
1

TABLE II

GEOMETRIC CHARACTERISTICS OF COMPONENT PARTS OF THE CONFIGURATIONS TESTED

Body:	
Maximum diameter, in.	7.00
Length of model with forebody extension, in.	96.00
Length of basic model, in.	87.00
Length of basic model, afterbody removed, in.	72.00
Fineness ratio of ogive section	4.29
Trapezoidal wing:	
Span, in.	45.64
Total area, sq ft	4.82
Exposed area, sq ft	3.61
Leading-edge sweep angle, deg	38.52
Trailing-edge sweep angle, deg	11.30
Aspect ratio	3.00
Taper ratio	0.14
Mean aerodynamic chord, in.	18.07
Airfoil section	NACA 65A006
Small canard surface - center-line position:	
Area, sq ft	0.77
Area, exposed, sq ft	0.41
Span (total), in.	18.26
Ratio of small-canard-surface area to wing area	0.16
Mean aerodynamic chord, in.	7.27
Airfoil section	NACA 65A006
Small canard surface - high position:	
Area, sq ft	0.77
Area, exposed, sq ft	0.62
Span, in.	18.26
Ratio of small-canard-surface area to wing area	0.16
Mean aerodynamic chord, in.	7.27
Airfoil section	Flat plate
Large canard surface:	
Area, sq ft	1.21
Area (exposed), sq ft	0.54
Span, in.	22.82
Ratio of large-canard-surface area to wing area	0.25
Mean aerodynamic chord, in.	9.03
Airfoil section	Flat plate
Vertical tail:	
Area exposed, sq ft	1.14
Span exposed, in.	14.06
Aspect ratio	1.21
Leading-edge sweep angle, deg	45.00
Horizontal-tail panel:	
Area, one panel exposed, sq ft	0.43
Span, one panel exposed, in.	5.70
Leading-edge sweep angle, deg	57.30

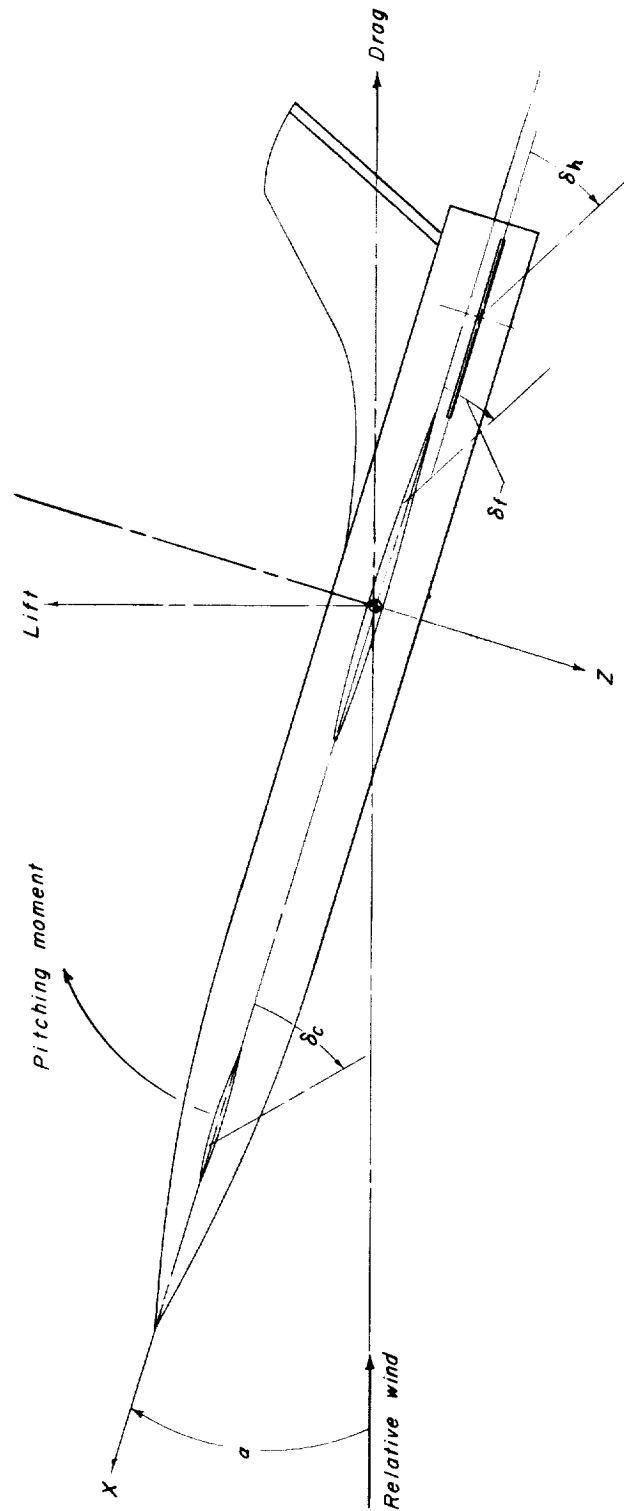
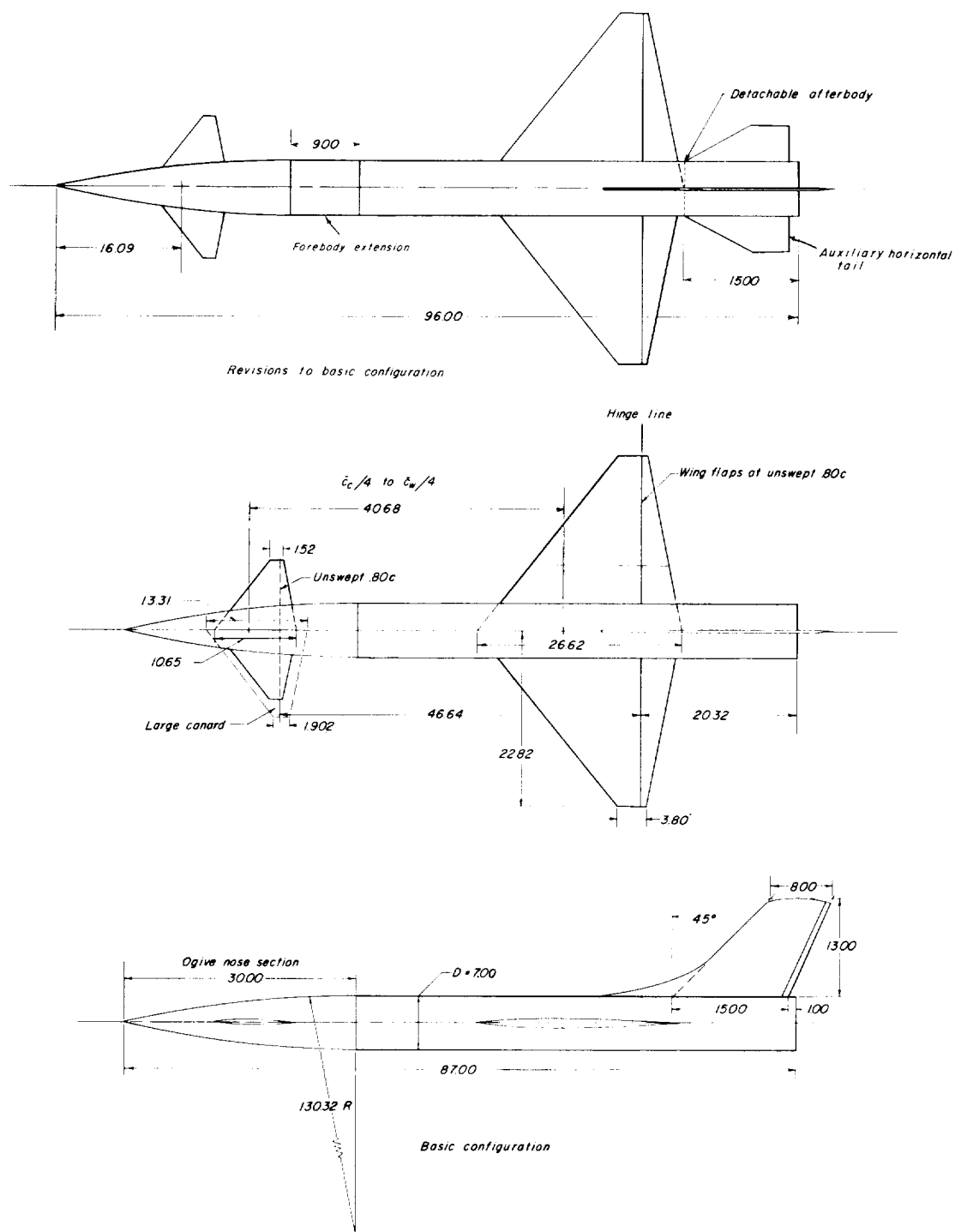
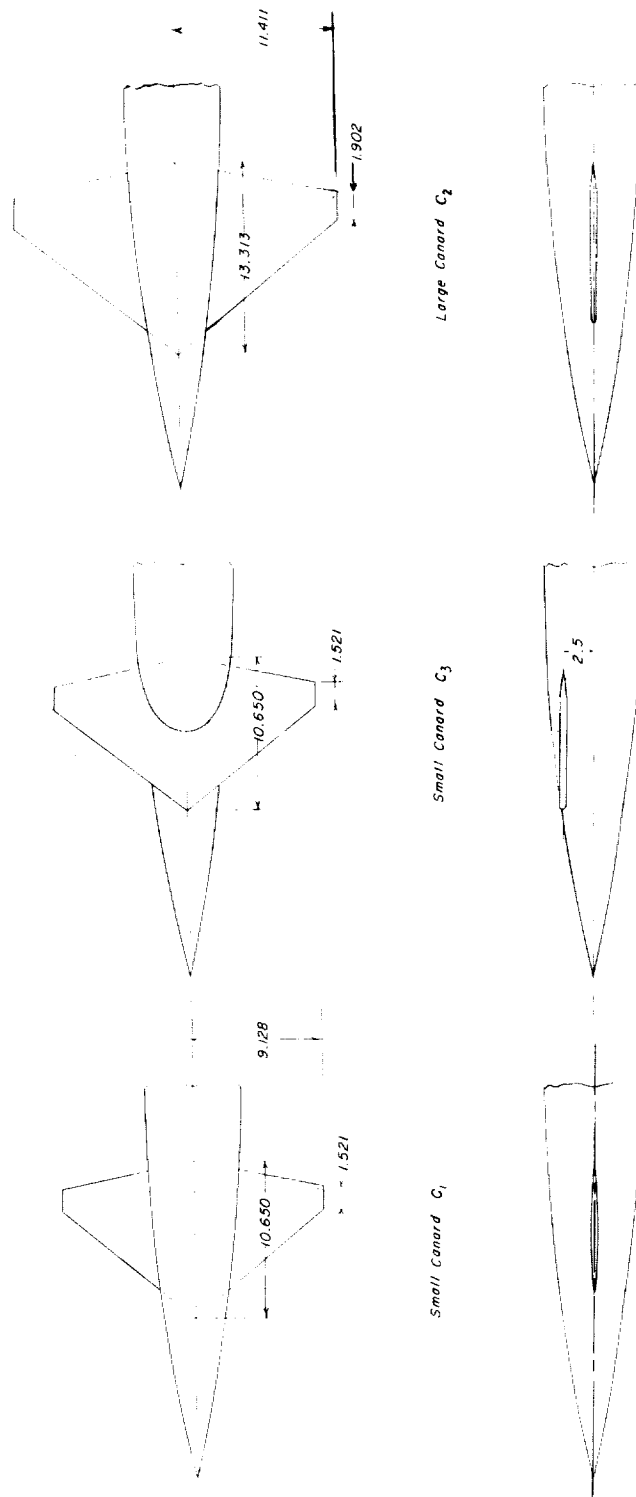


Figure 1.- Body reference axes showing positive directions of lift, drag, pitching moment, and angular deflections.



(a) Basic configuration and revisions of extended fuselage and auxiliary horizontal tail.

Figure 2.- Geometric characteristics of canard configuration. (All dimensions are in inches.)



(b) Relative locations of the three canard surfaces tested.

Figure 2.- Concluded.

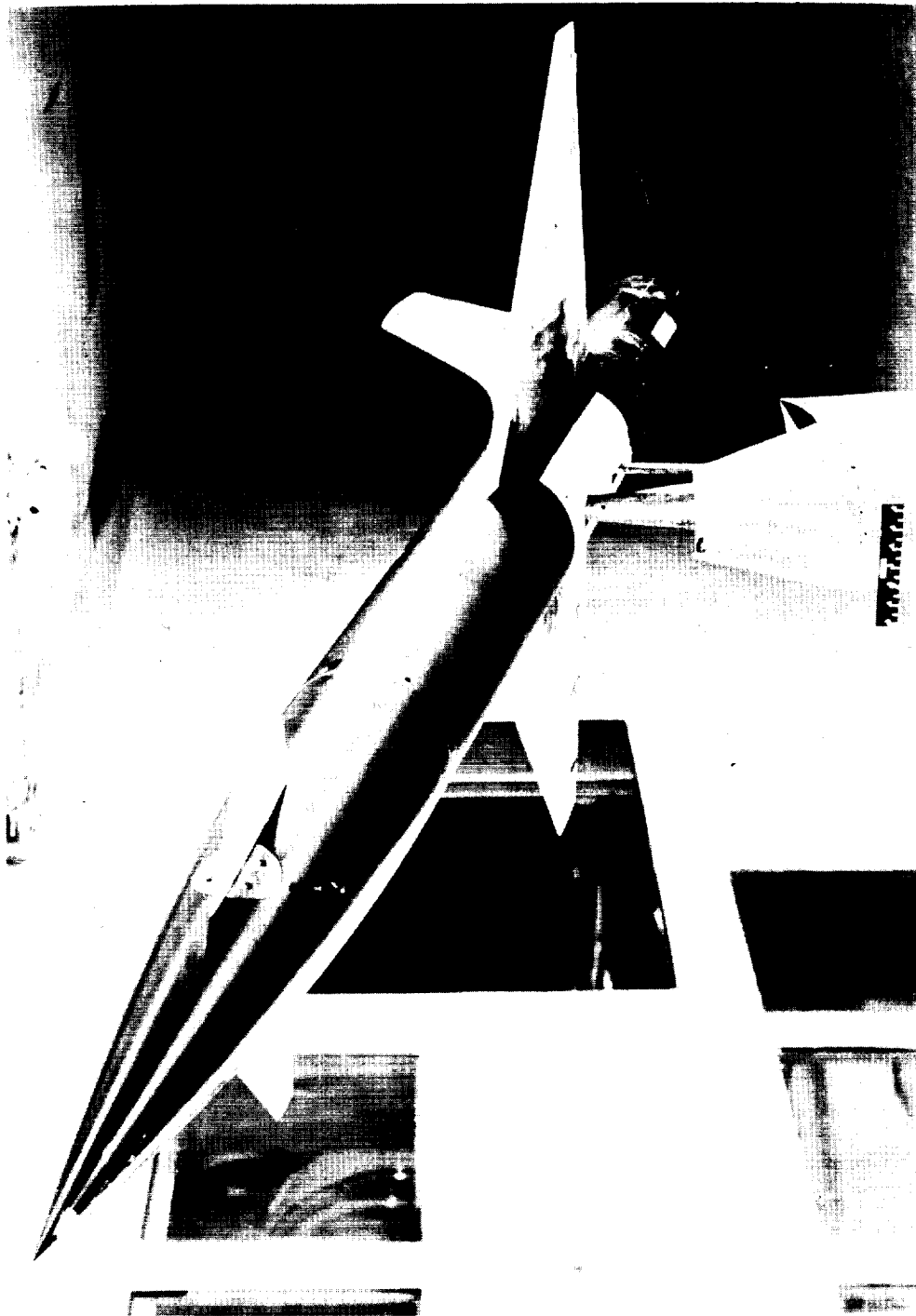


Figure 3.- Photograph of the basic model with small canard surface installed in the
Langley 300-MPH 7- by 10-foot tunnel.

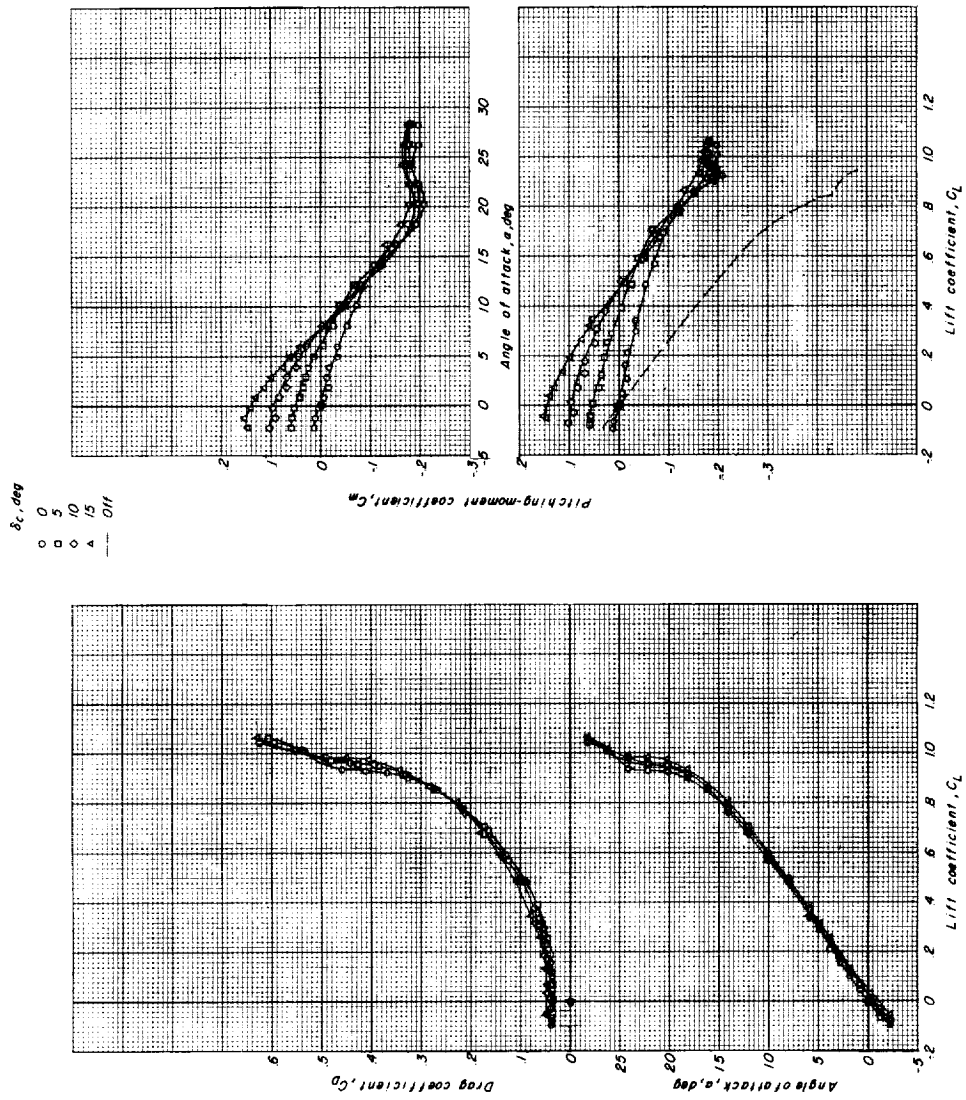
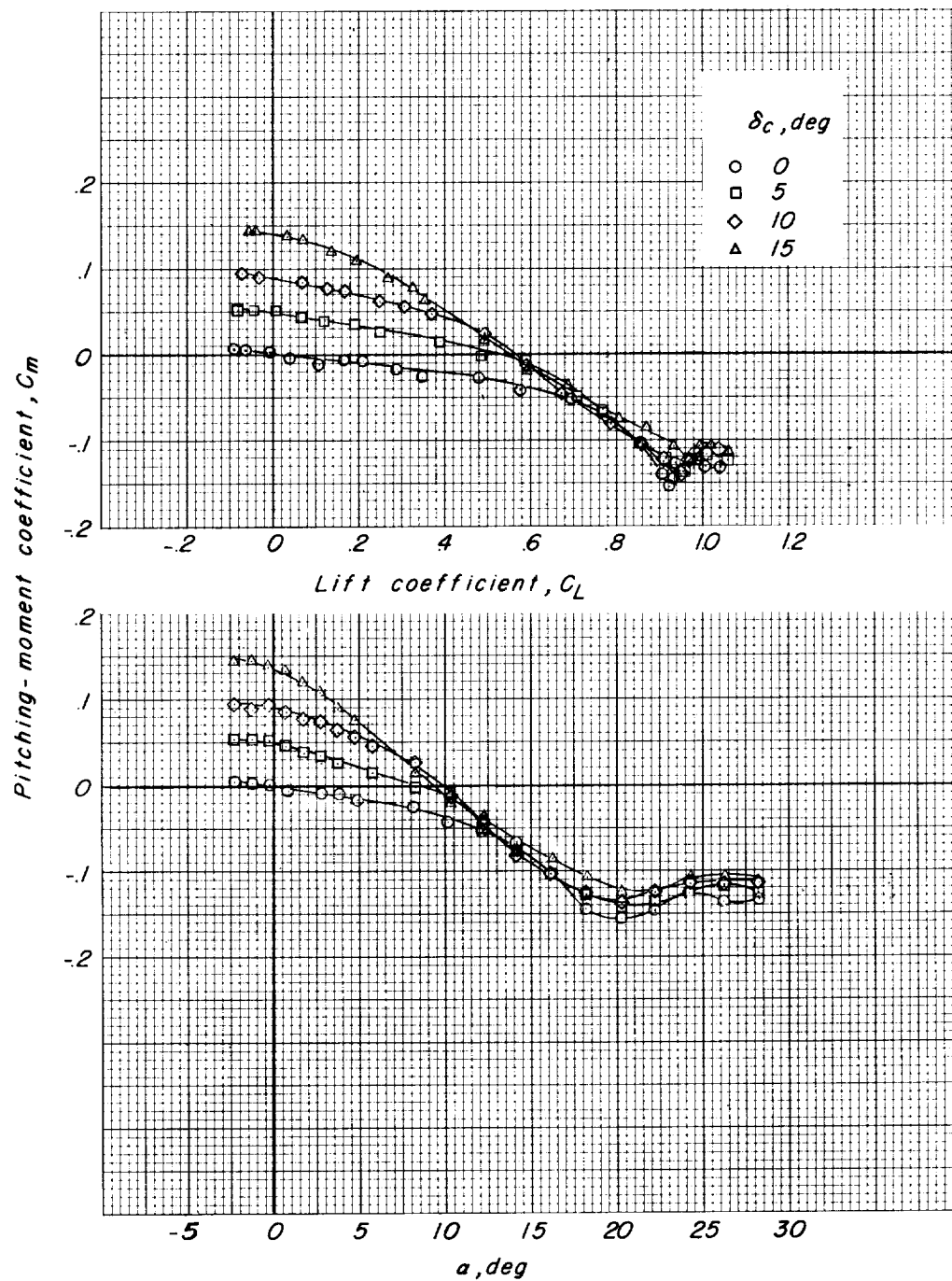


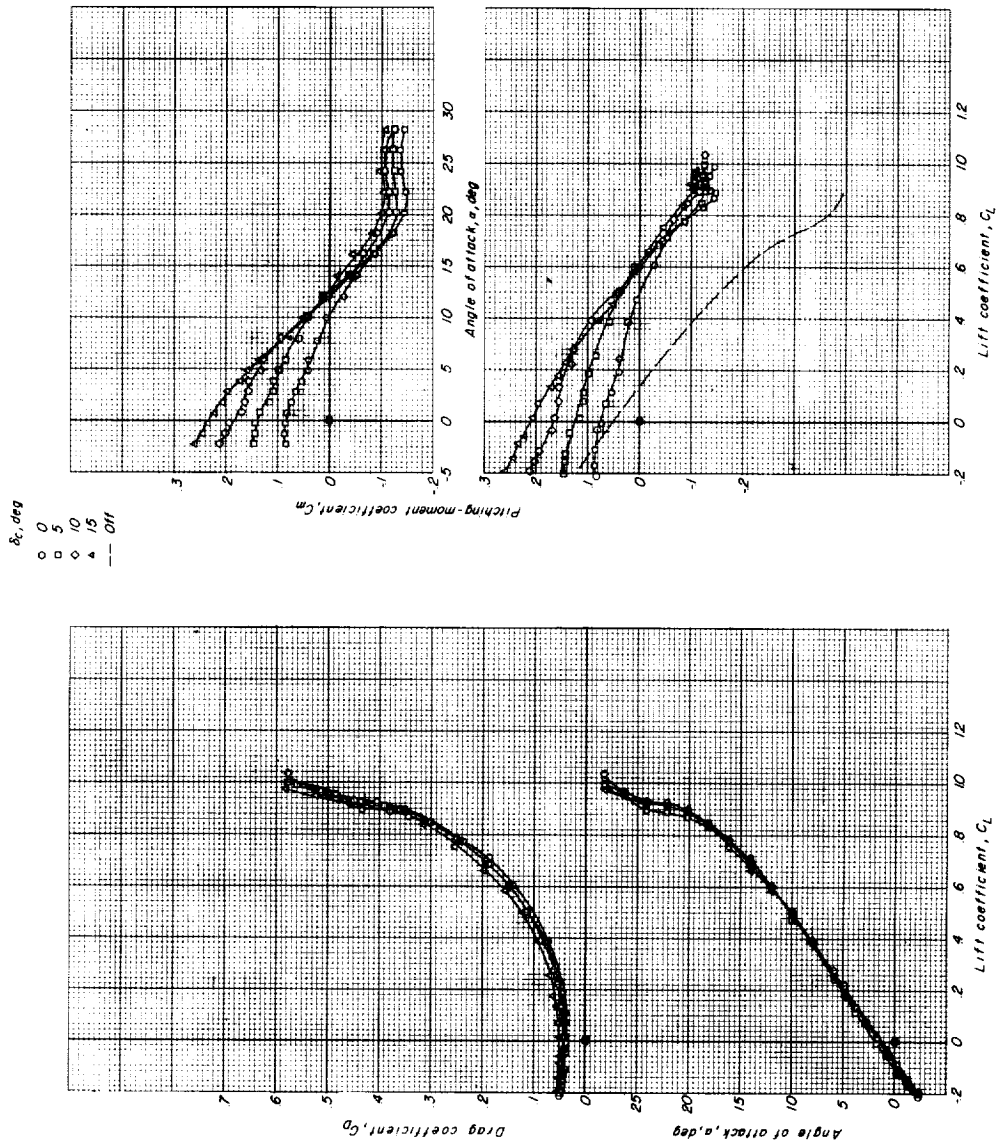
Figure 4.- Effects of deflections of the small canard surface on the aerodynamic characteristics in pitch. WFAC₁.

L-221



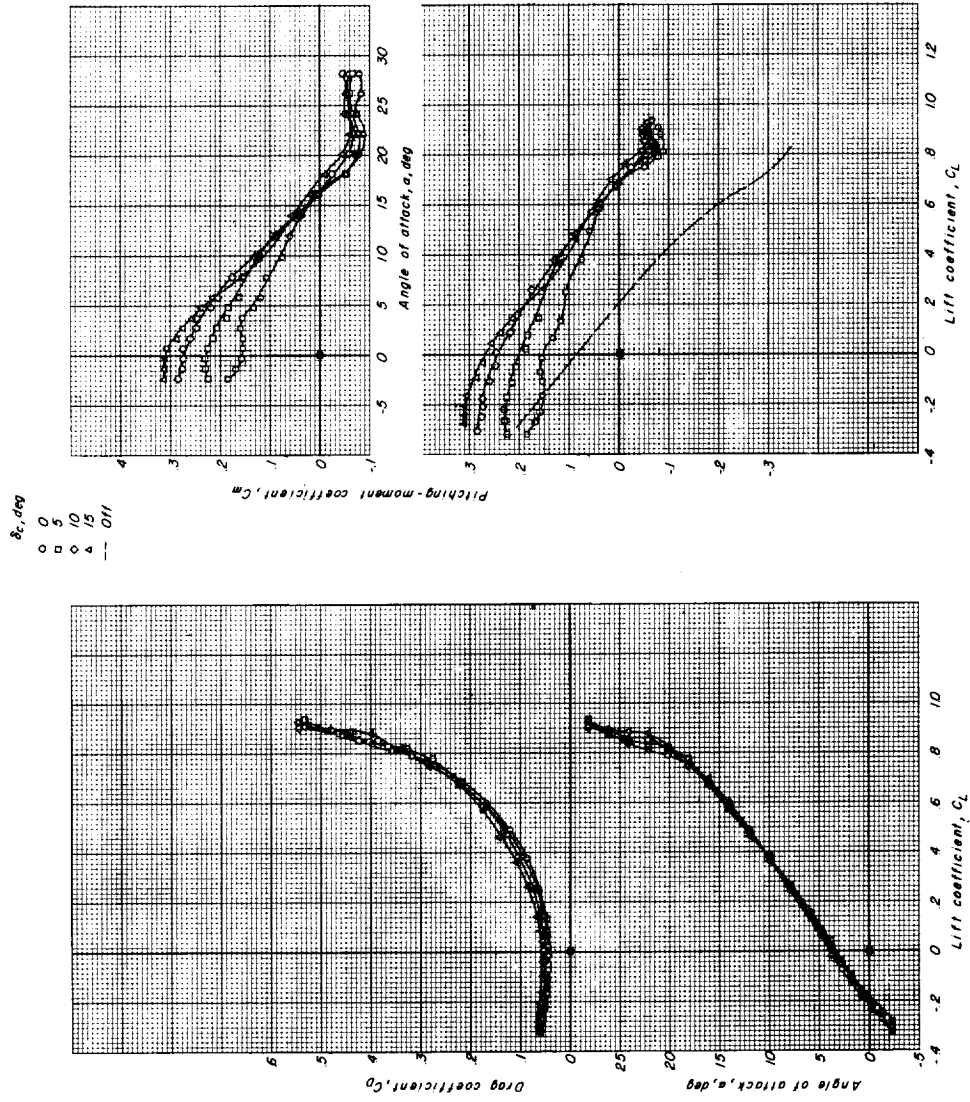
(b) $\delta_f = 0^\circ$. Moment reference located $0.37\bar{c}_w$ ahead of $\frac{\bar{c}_w}{4}$.

Figure 4.- Continued.



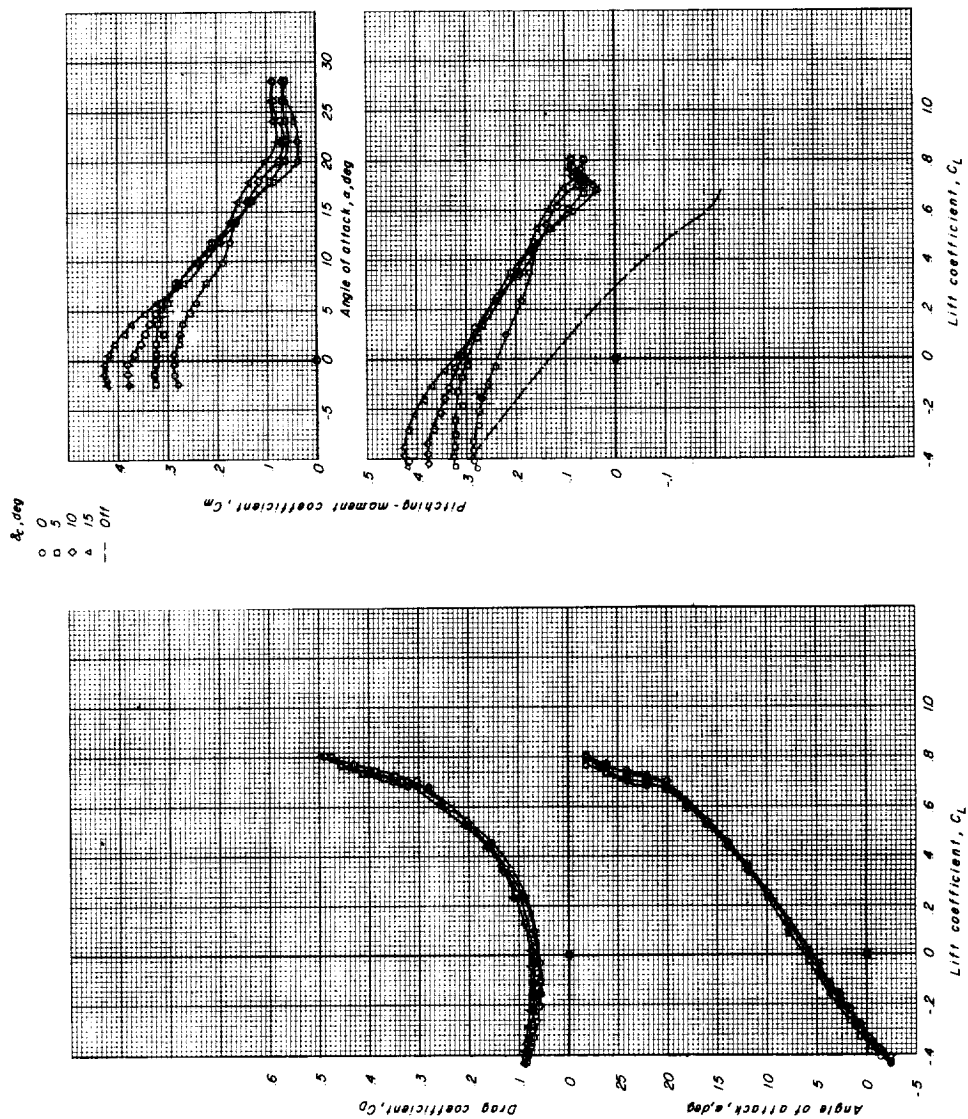
(c) $\delta_f = -5^\circ$. Moment reference located $0.42\bar{c}_w$ ahead of $\frac{\bar{c}_w}{4}$.

Figure 4.- Continued.



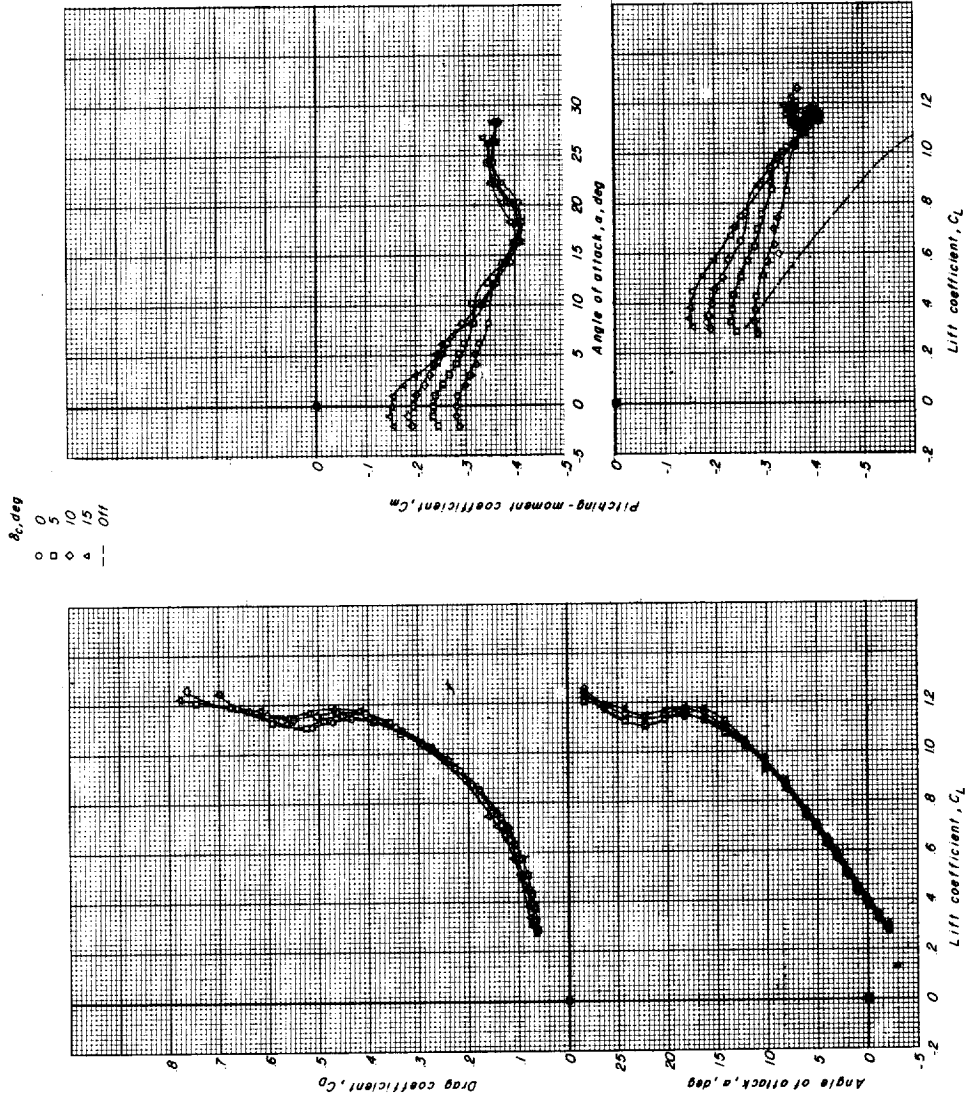
(d) $\delta_f = -10^\circ$. Moment reference located $0.42\bar{c}_w$ ahead of $\frac{\bar{c}_w}{4}$.

Figure 4.- Continued.



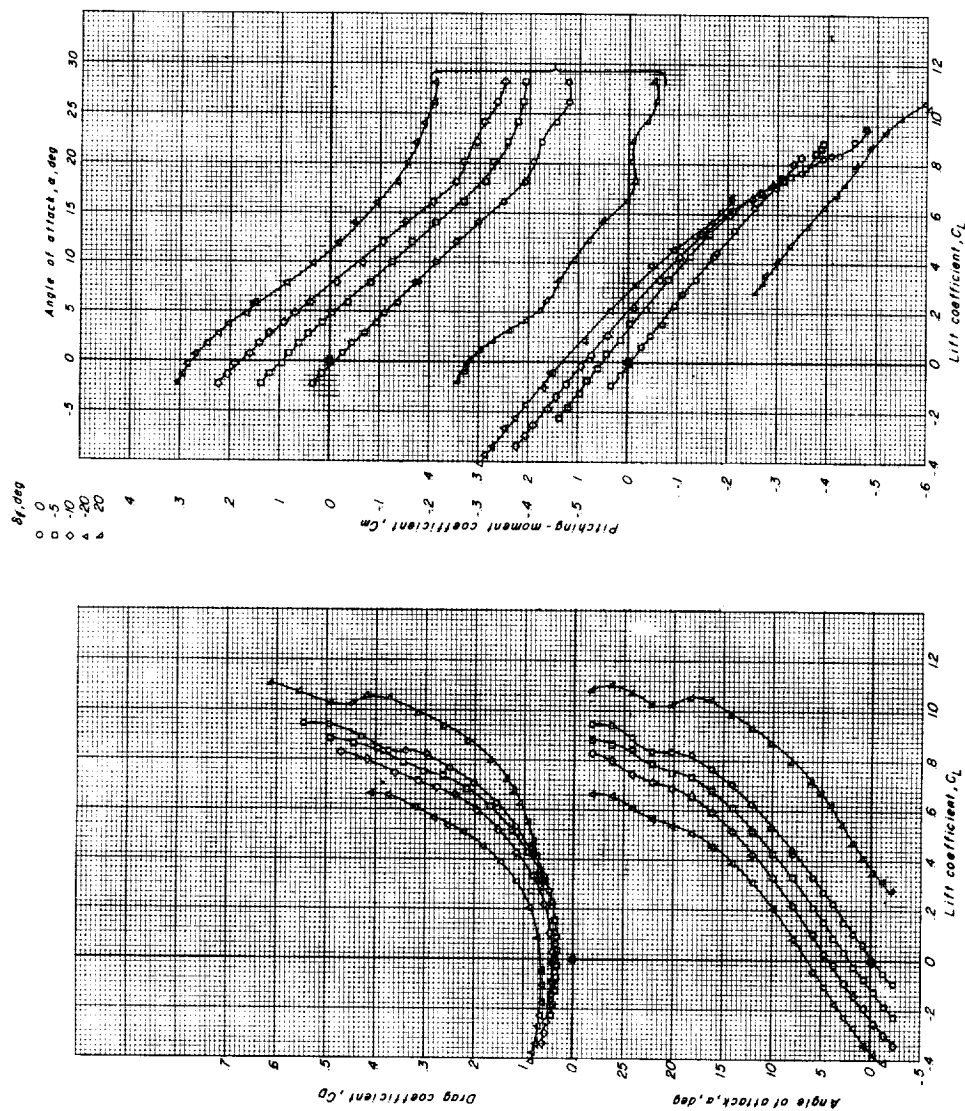
(e) $\delta_f = -20^\circ$. Moment reference located $0.42\bar{c}_w$ ahead of $\frac{\bar{c}_w}{4}$.

Figure 4.- Continued.



(f) $\delta_f = 20^\circ$. Moment reference located $0.42\bar{c}_w$ ahead of $\frac{\bar{c}_w}{4}$.

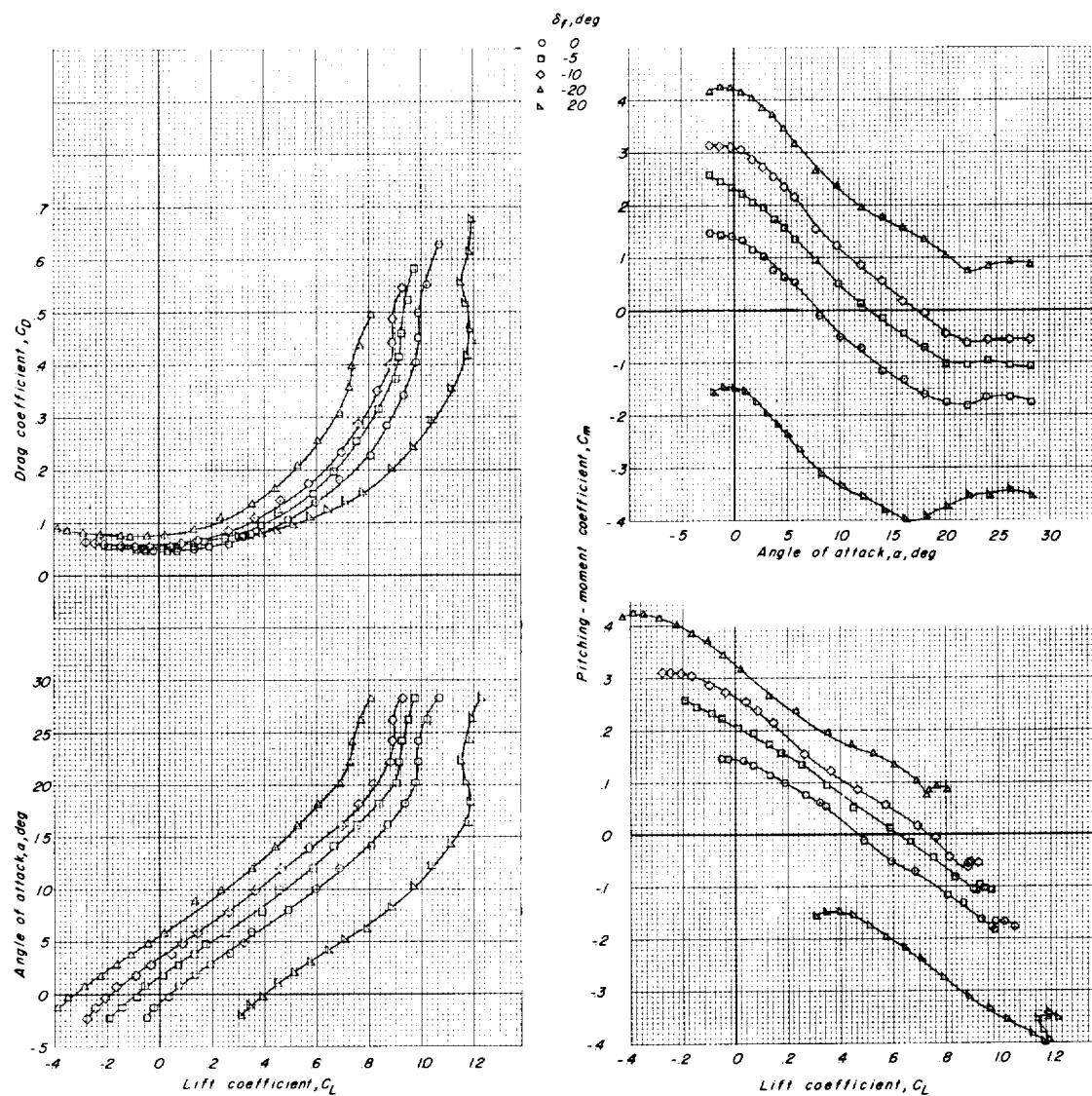
Figure 4.- Concluded.



(a) Small canard surface off (WFA).

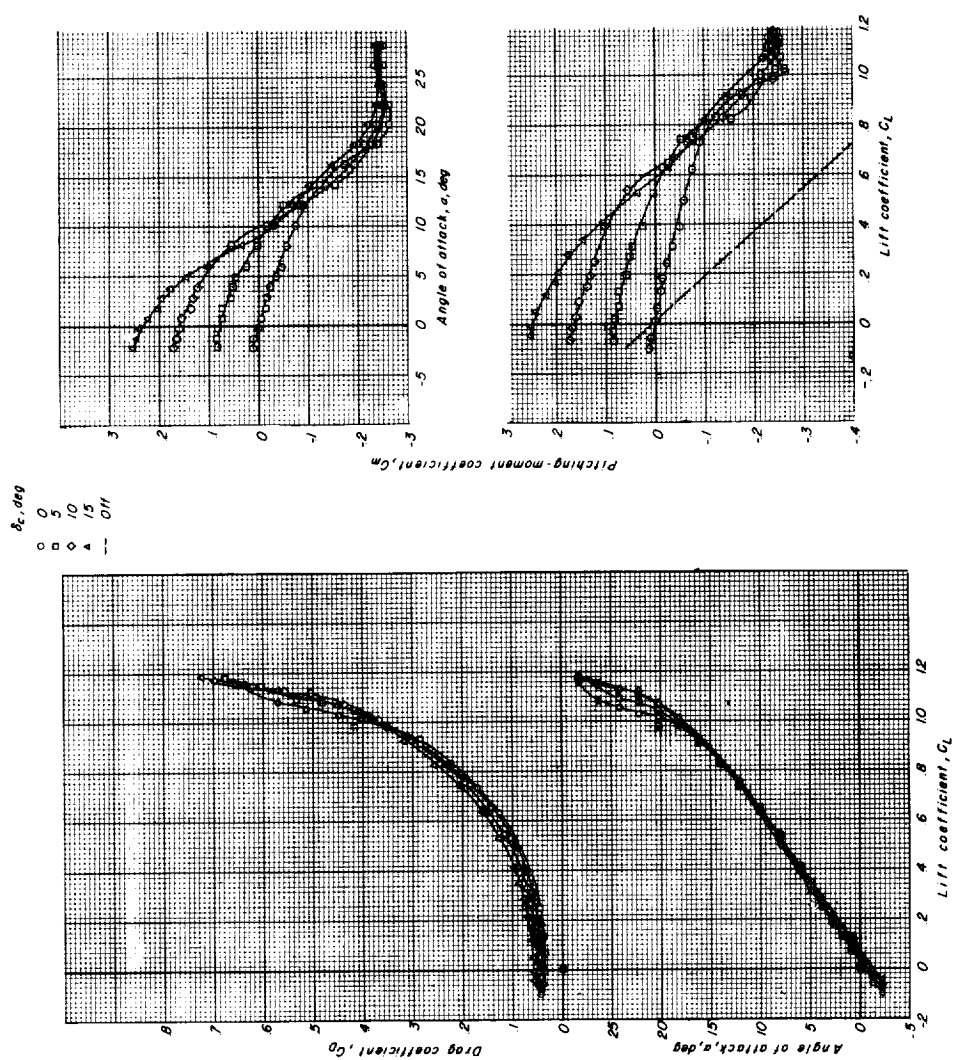
Figure 5.- Effects of the wing trailing-edge flap control deflections on the aerodynamic characteristics in pitch of the basic configuration. Moment reference located $0.42\bar{c}_w$ ahead of $\frac{\bar{c}_w}{4}$.

L-221



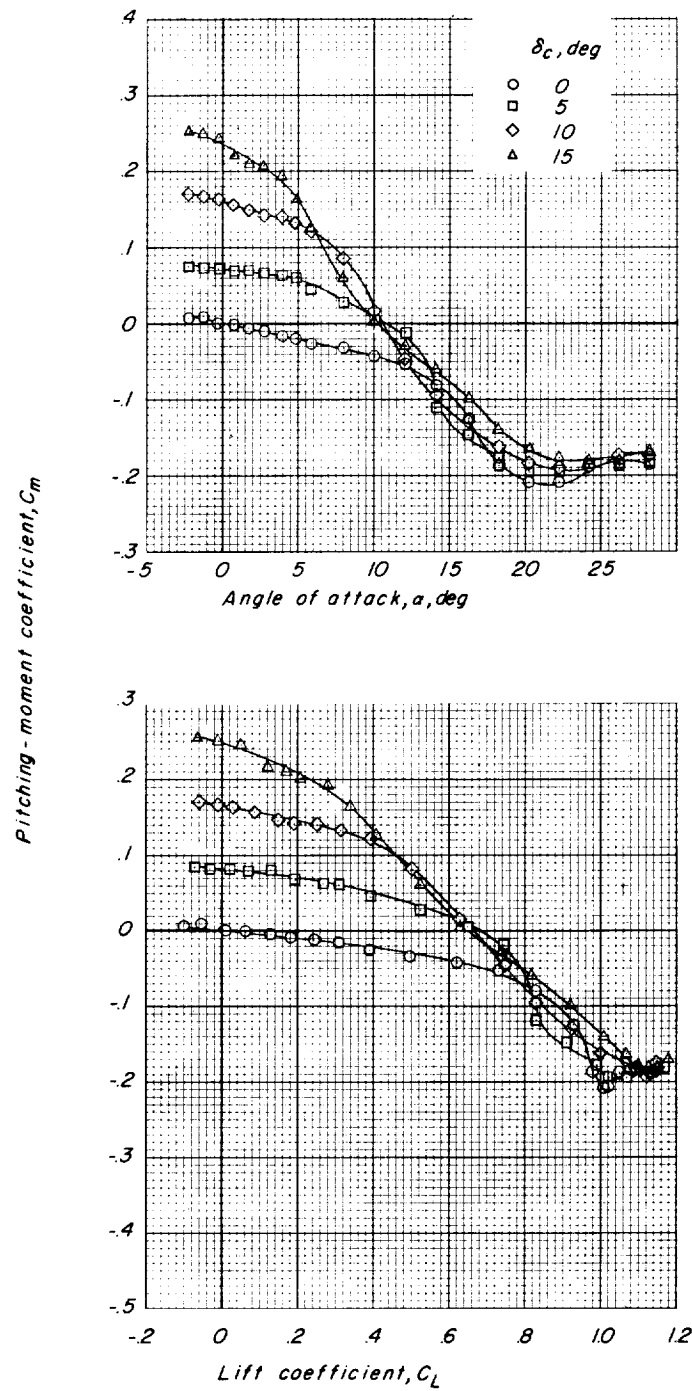
(b) Small canard surface on (WFAC₁). $\delta_c = 15^\circ$.

Figure 5.- Concluded.



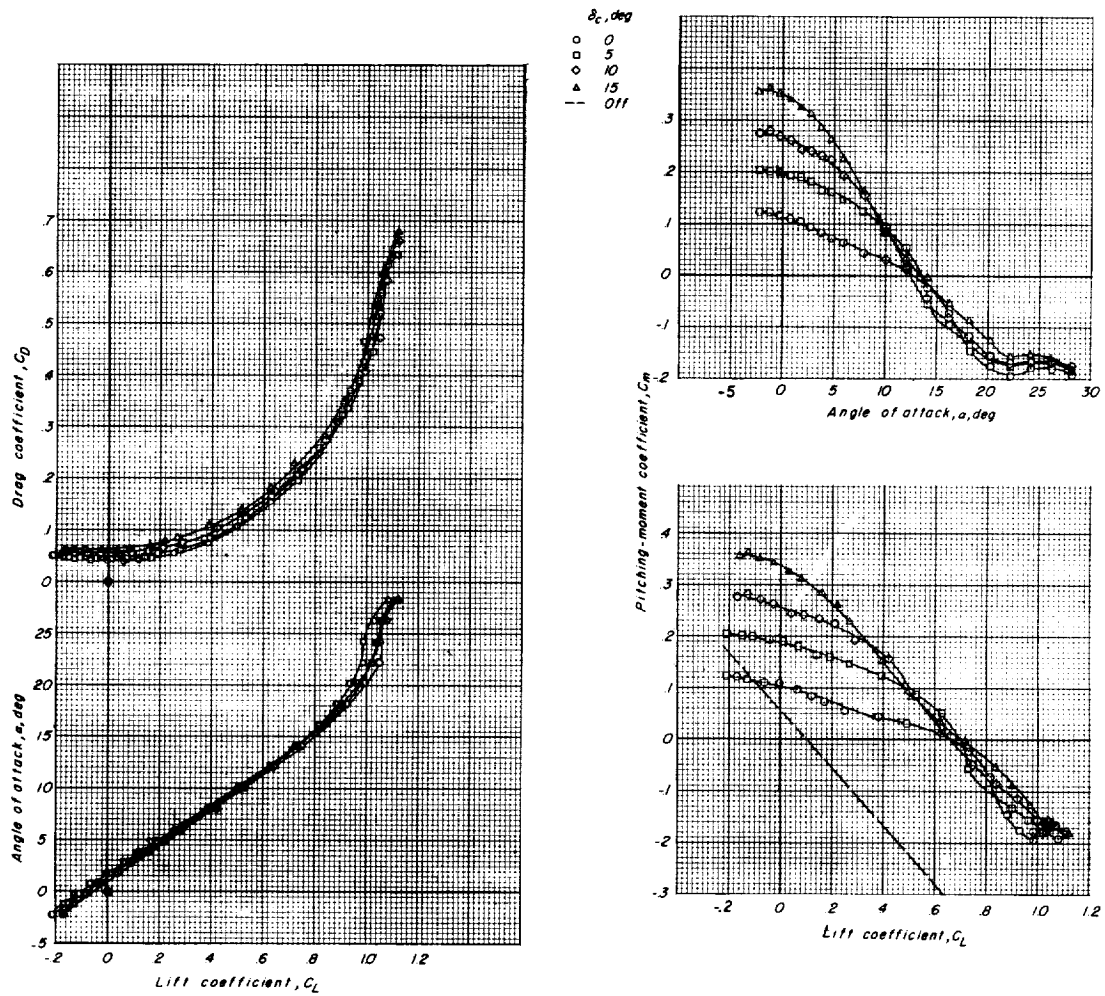
(a) $\delta_f = 0^\circ$. Moment reference located $0.59\bar{c}_w$ ahead of $\frac{\bar{c}_w}{4}$.
 Effects of deflection of the large canard surface on aerodynamic characteristics in pitch. WFAC₂.

L-221



(b) $\delta_f = 0^\circ$. Moment reference located $0.54\bar{c}_w$ ahead of $\frac{\bar{c}_w}{4}$.

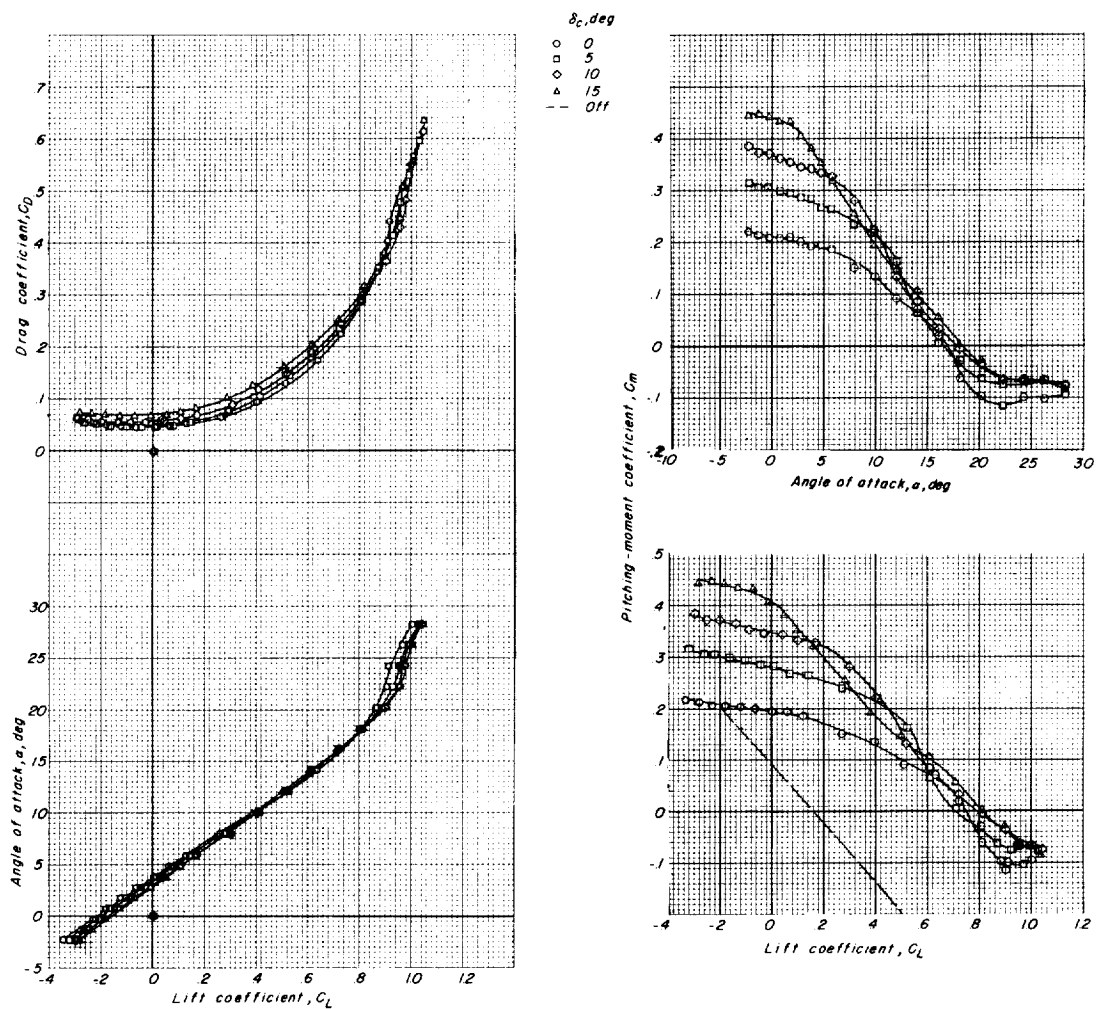
Figure 6.- Continued.



(c) $\delta_F = -5^\circ$. Moment reference located $0.59\bar{c}_w$ ahead of $\frac{\bar{c}_w}{4}$.

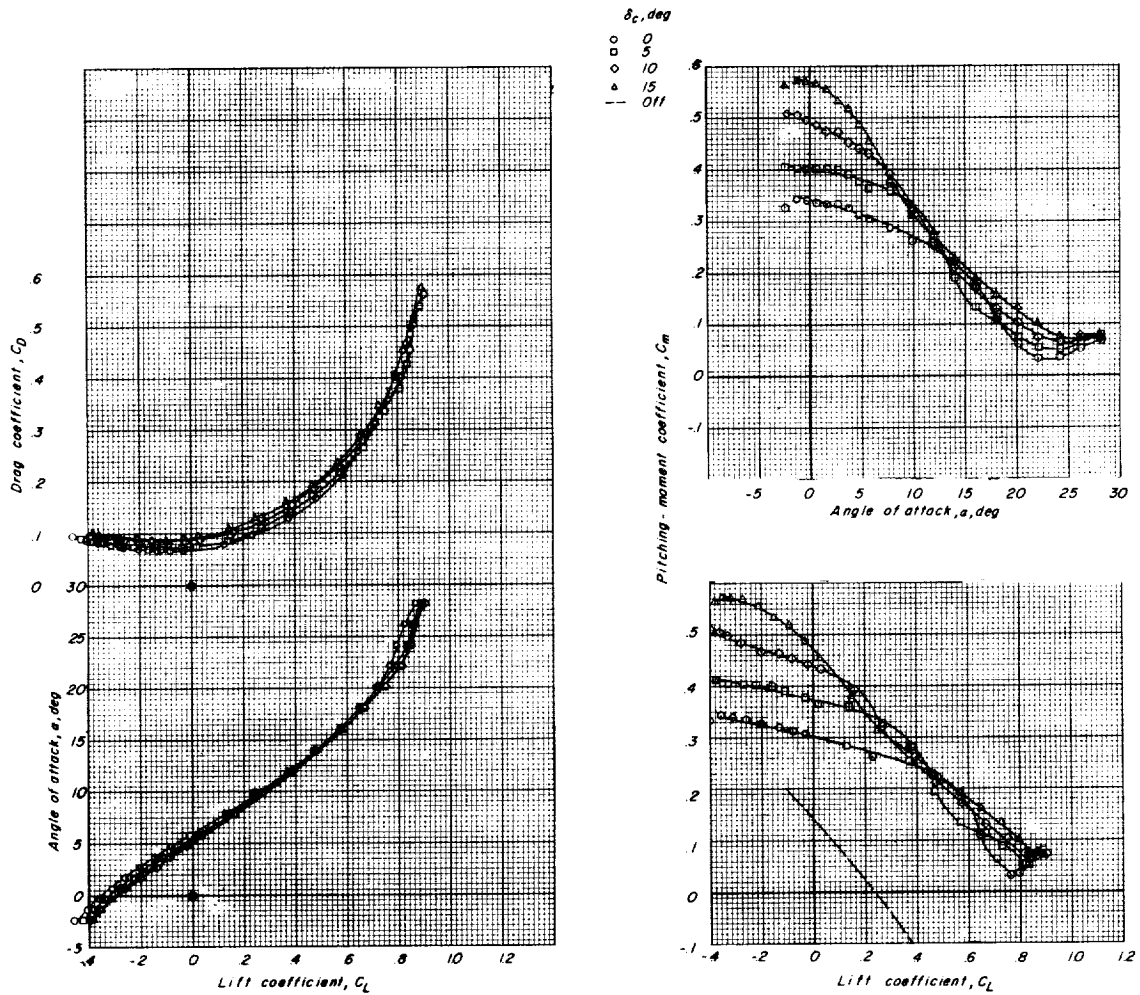
Figure 6.- Continued.

L-221



(d) $\delta_F = -10^\circ$. Moment reference located $0.59\bar{c}_w$ ahead of $\frac{\bar{c}_w}{4}$.

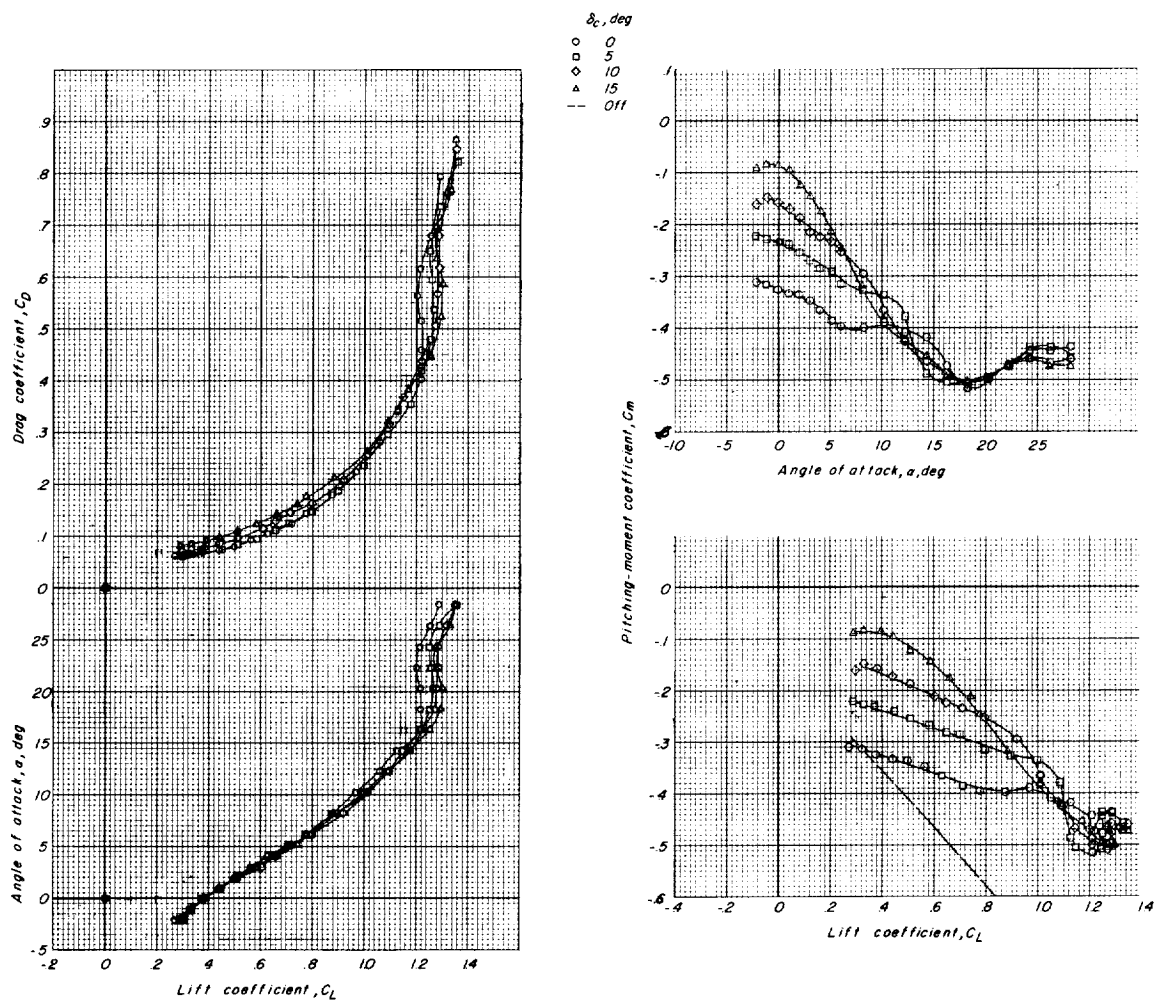
Figure 6.- Continued.



(e) $\delta_f = -20^\circ$. Moment reference located $0.59\bar{c}_w$ ahead of $\frac{\bar{c}_w}{4}$.

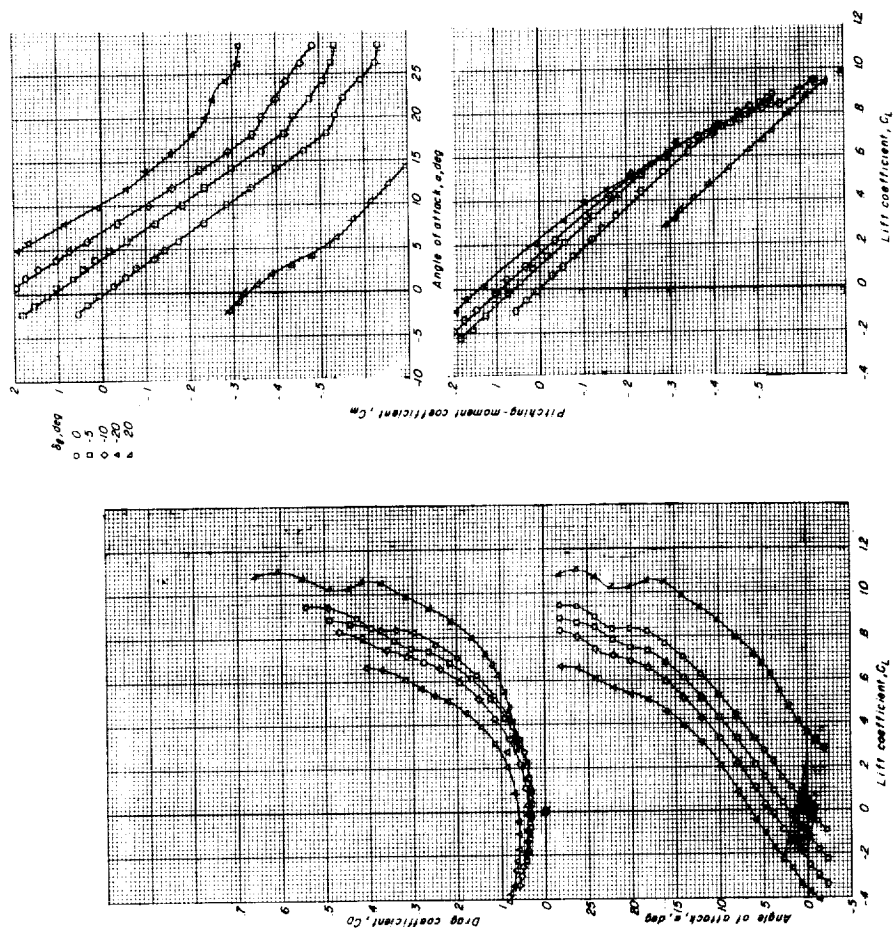
Figure 6.- Continued.

L-221



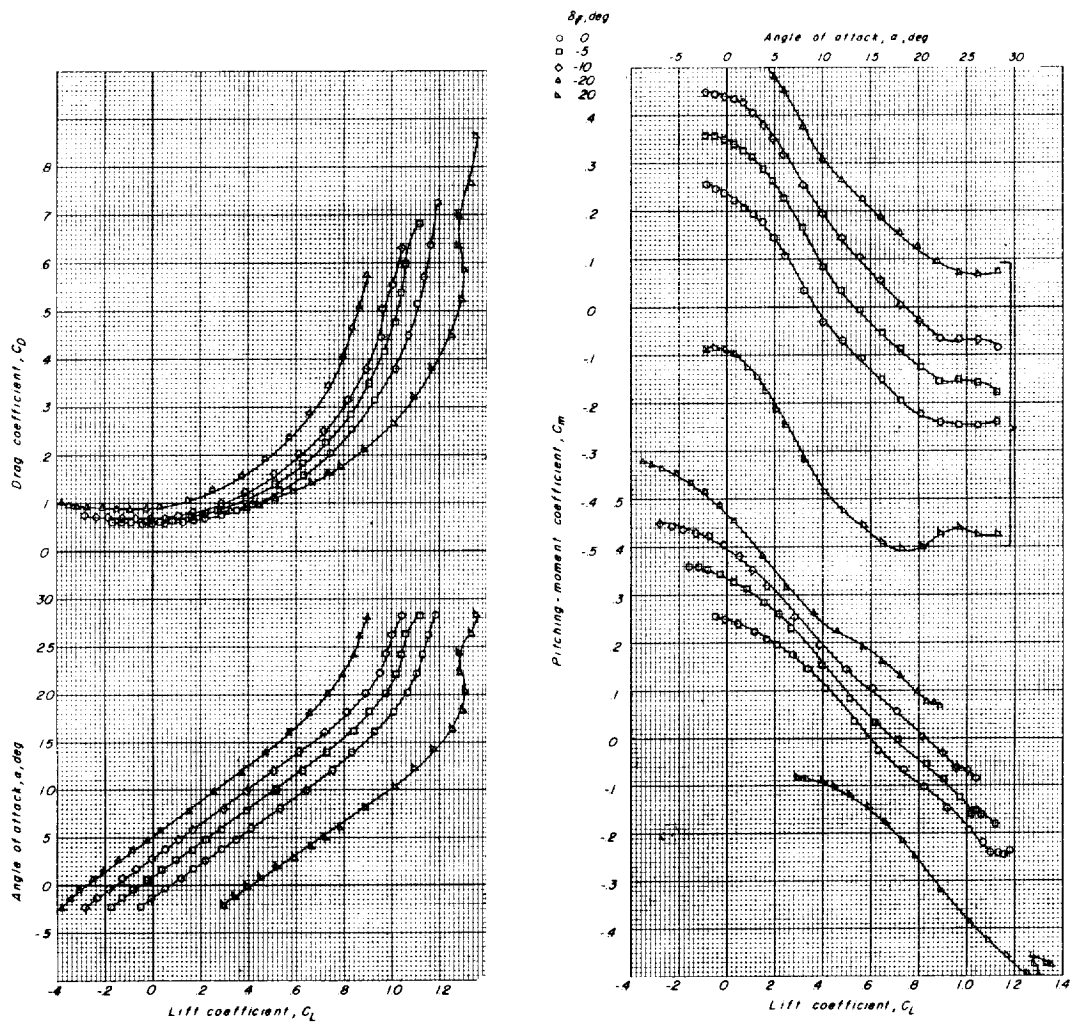
(f) $\delta_f = 20^\circ$. Moment reference located $0.59\bar{c}_w$ ahead of $\frac{\bar{c}_w}{4}$.

Figure 6.- Concluded.



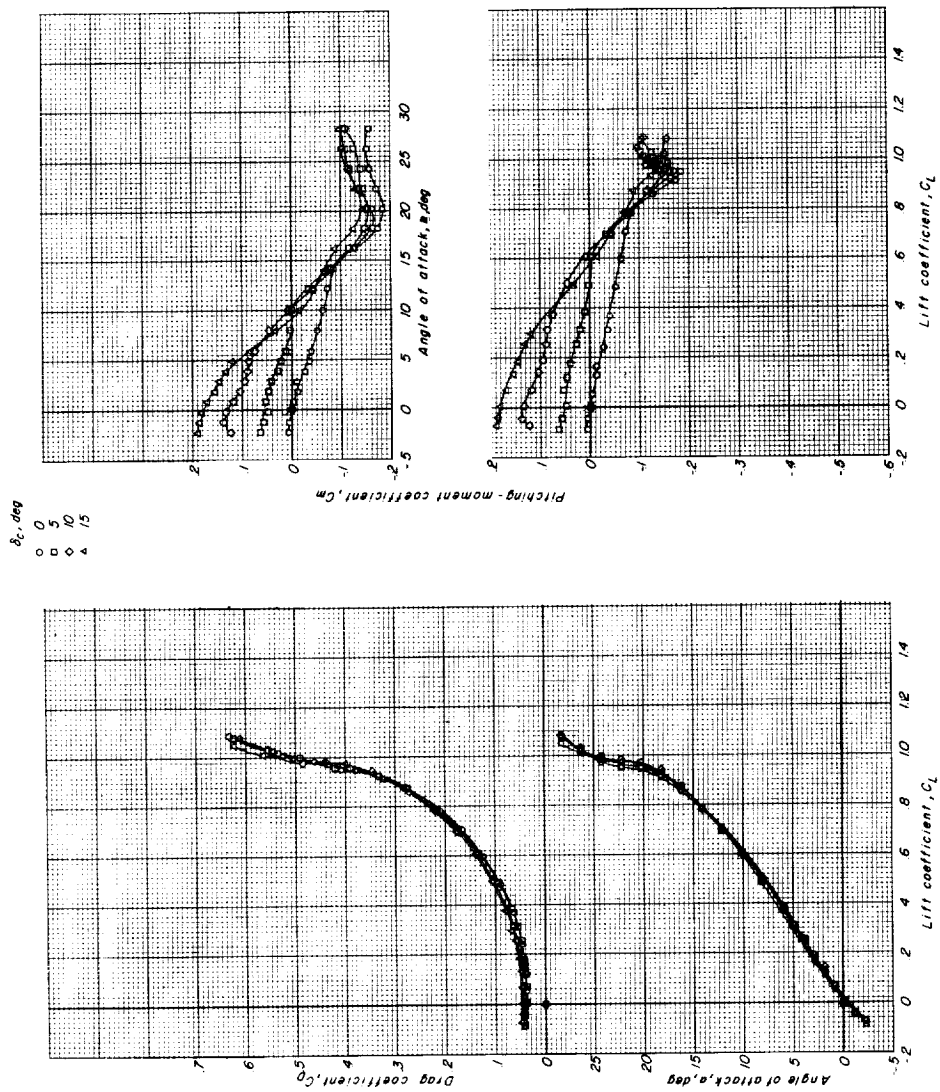
(a) Large canard surface off (WFA).

Figure 7.- Effects of the wing trailing-edge flap control deflections on the aerodynamic characteristics in pitch of the basic configuration. Moment reference located $0.59\bar{c}_w$ ahead of $\frac{\bar{c}_w}{4}$.



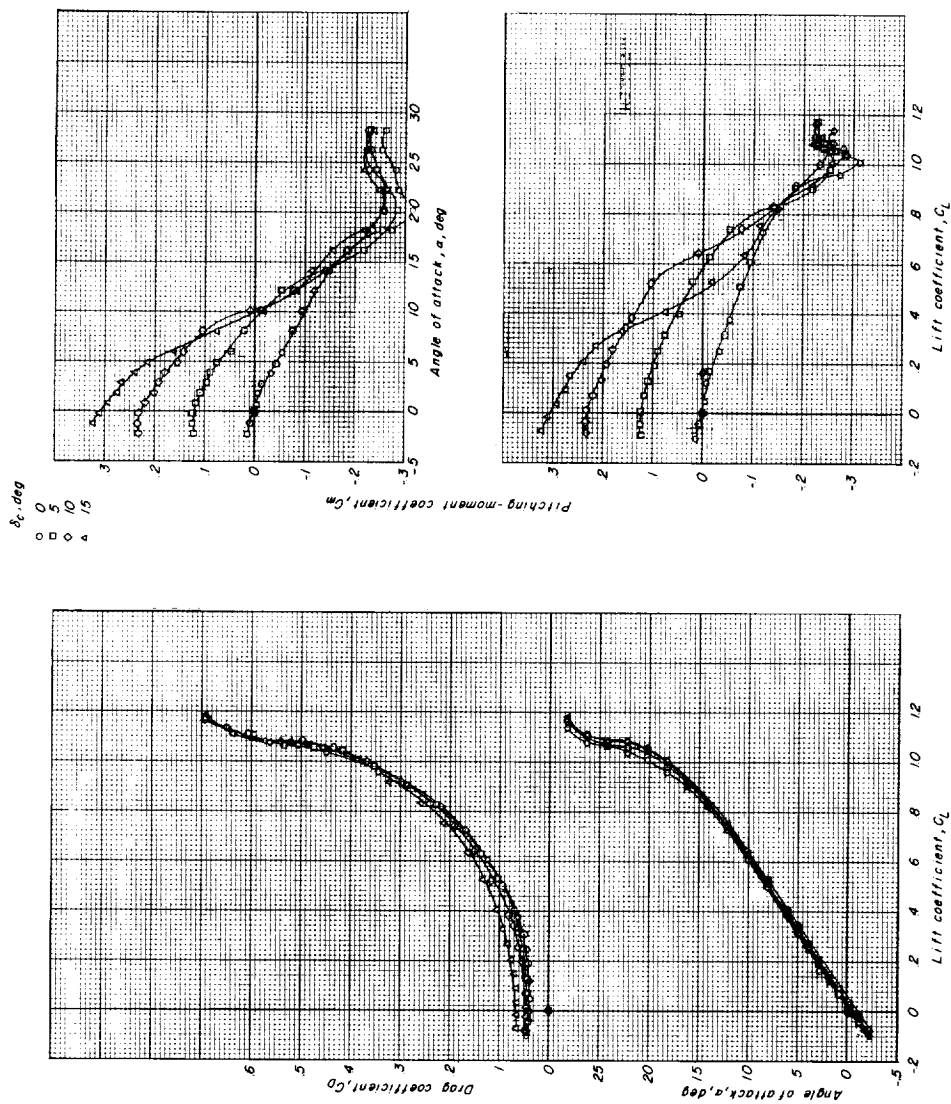
(b) Large canard surface on (WFAC₂). $\delta_c = 15^\circ$.

Figure 7.- Concluded.



(a) Small canard surface on (WFAEC₁) ($\frac{\bar{c}_w}{4}$). Moment reference located $0.48\bar{c}_w$ ahead of the configuration with fuselage forebody extended. $\delta_f = 0^\circ$.

Figure 8.- Effects of canard-surface deflections on the aerodynamic characteristics in pitch of the configuration with fuselage forebody extended. $\delta_f = 0^\circ$.



(b) Large canard surface on (WFAEC₂). Moment reference located 0.70 \bar{c}_w ahead of $\frac{\bar{c}_w}{4}$.

Figure 8.- Concluded.

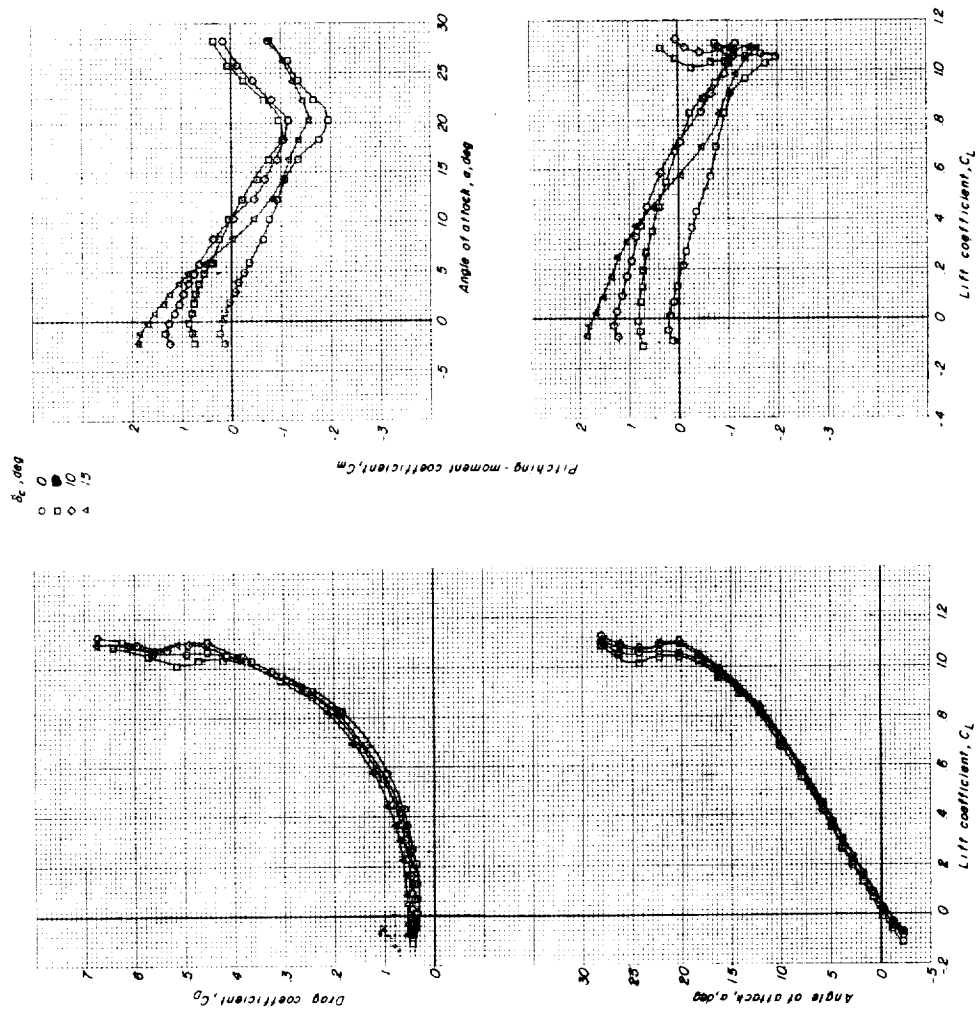


Figure 9.- Effects of small-canard-surface deflections on the aerodynamic characteristics in pitch of model with afterbody removed. Moment reference located $0.42\bar{c}_w$ ahead of $\frac{\bar{c}_w}{4}$.

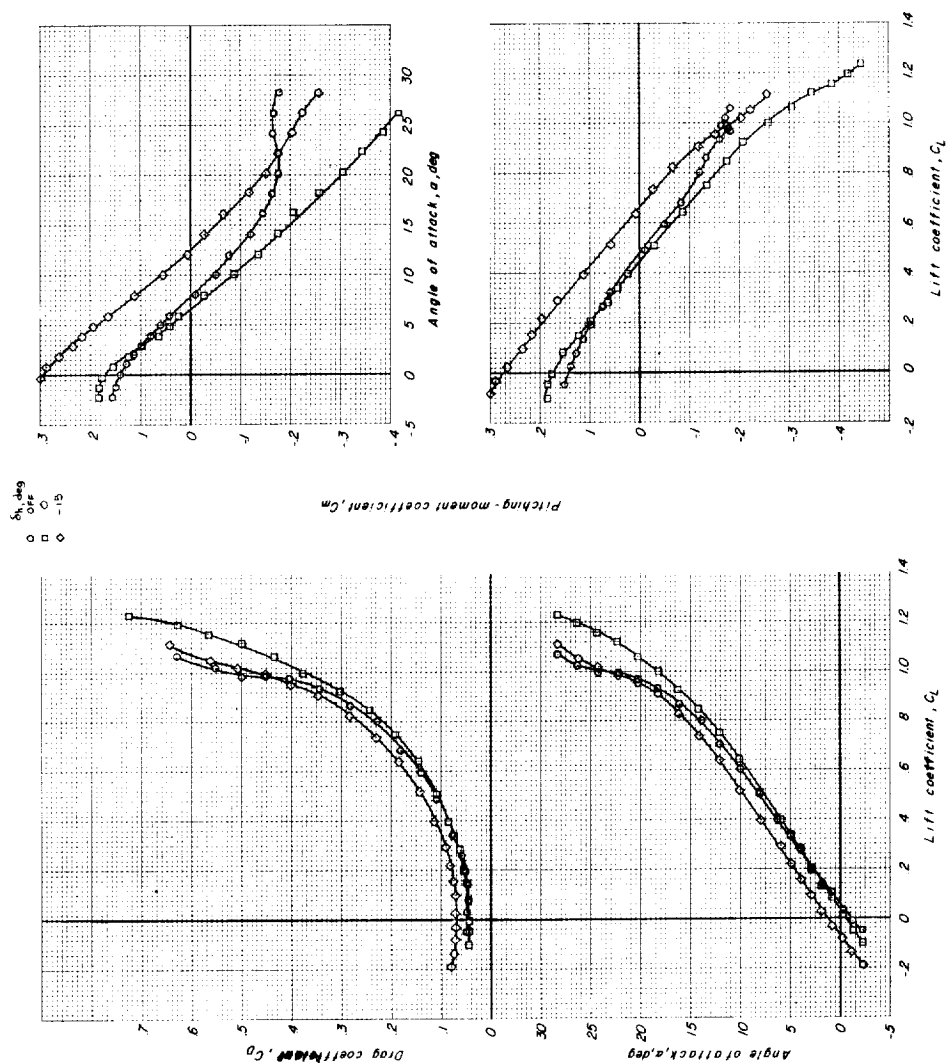
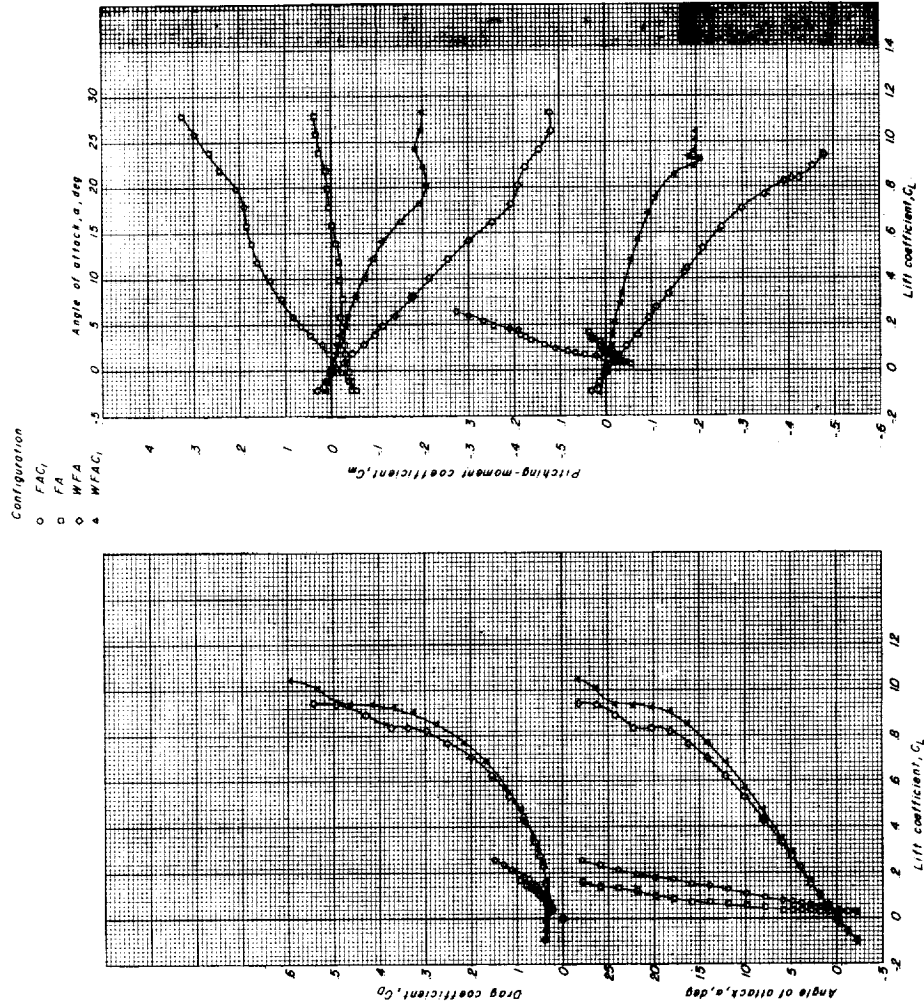
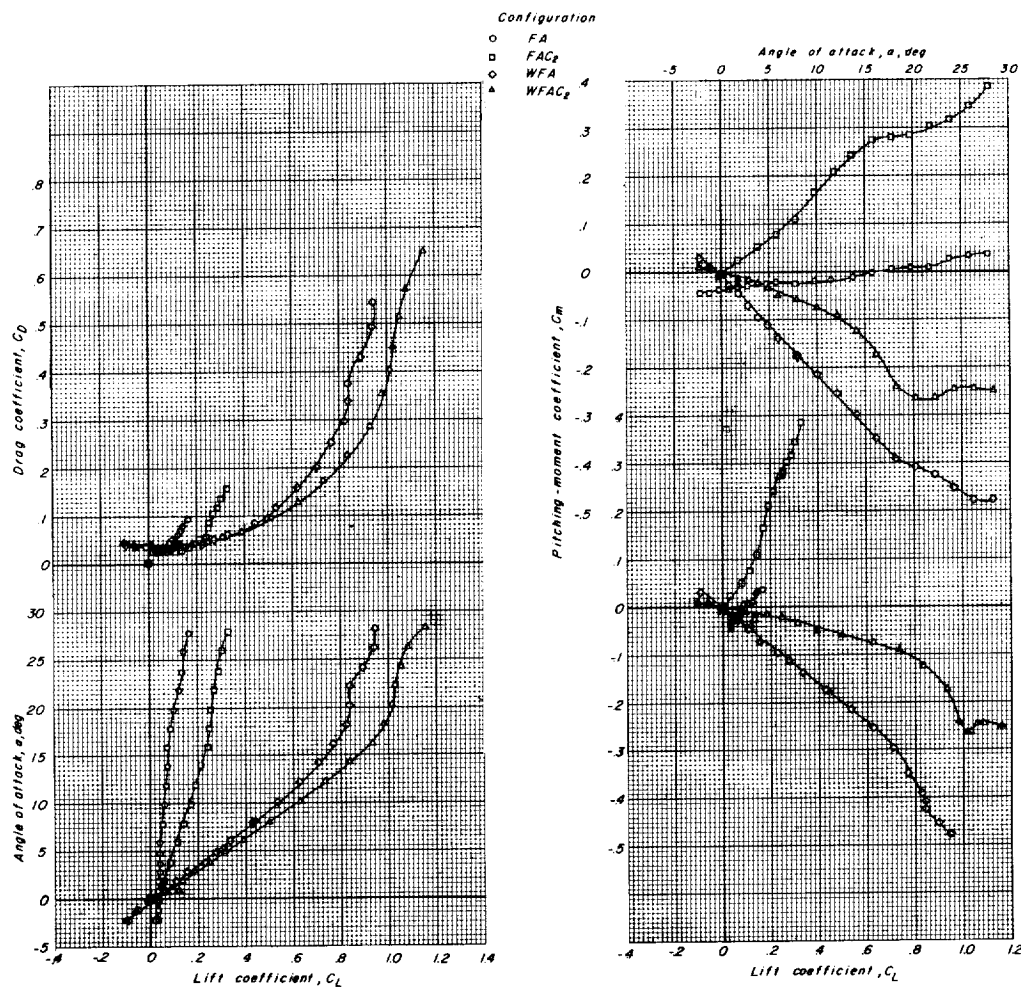


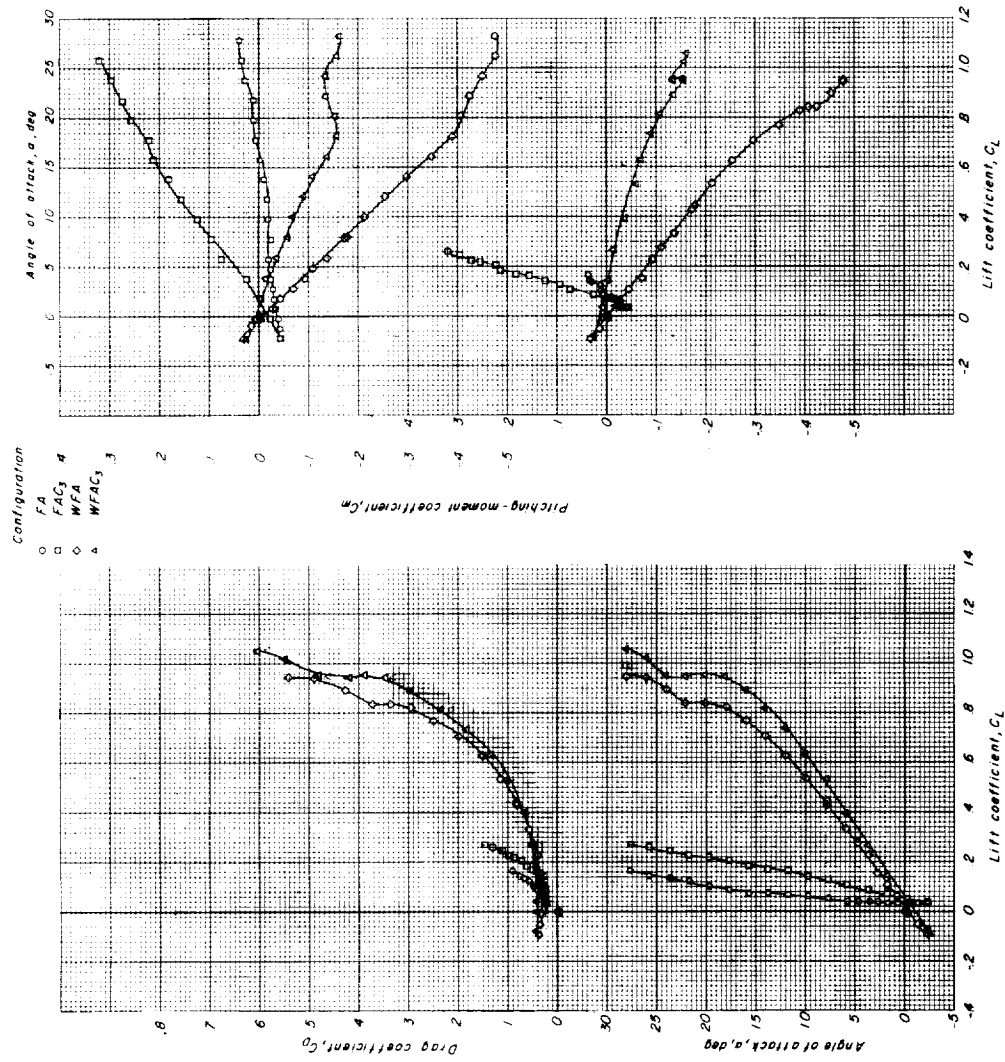
Figure 10.- Effects of the addition of auxiliary horizontal tail to basic configuration on the aerodynamic characteristics in pitch. Moment reference located $0.42\bar{c}_w$ ahead of $\frac{\bar{c}_w}{4}$. $\delta_c = 15^\circ$; $\delta_f = 0^\circ$.





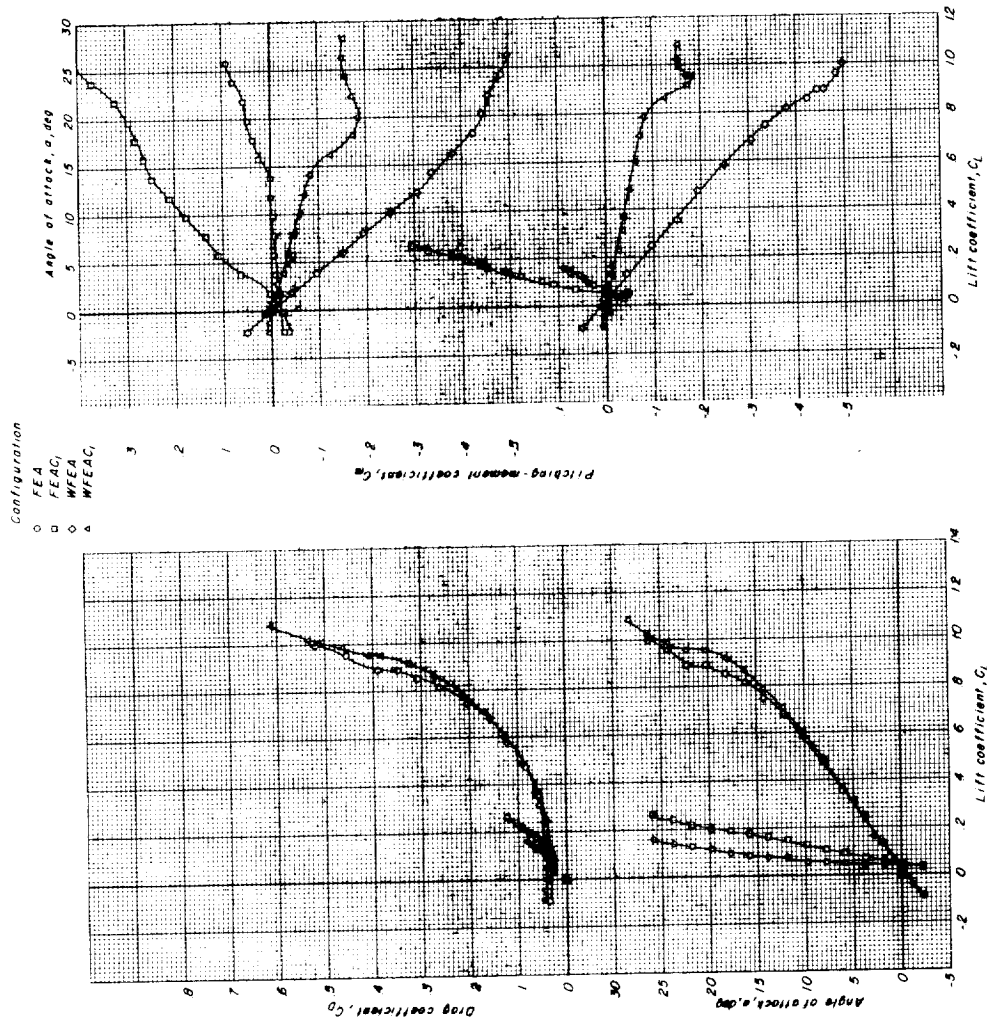
(b) Large canard surface. Moment reference located $0.59\bar{c}_w$ ahead of $\frac{\bar{c}_w}{4}$.

Figure 11.- Continued.



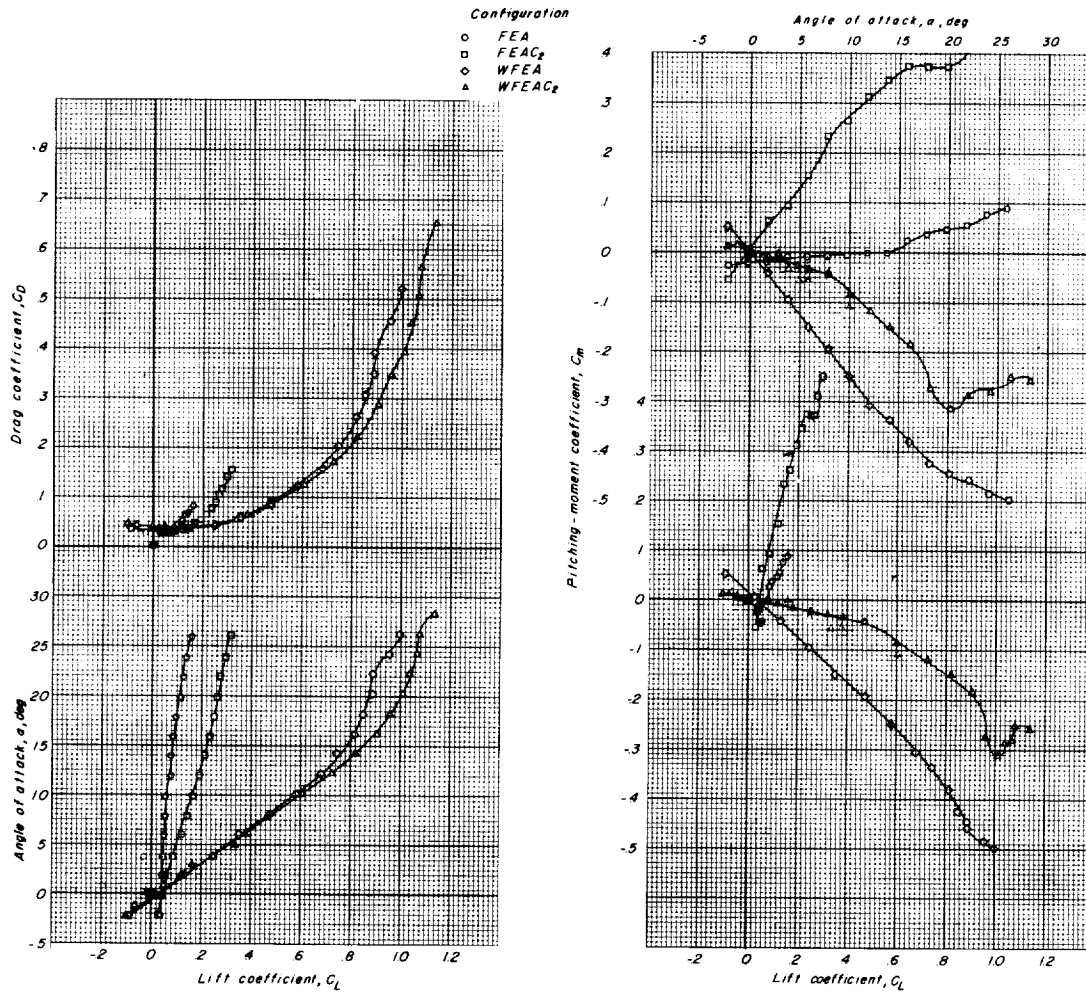
(c) Small canard surface in high position. Moment reference located at $0.42\bar{c}_w$ ahead of \bar{c}_w .

Figure 11.- Concluded.



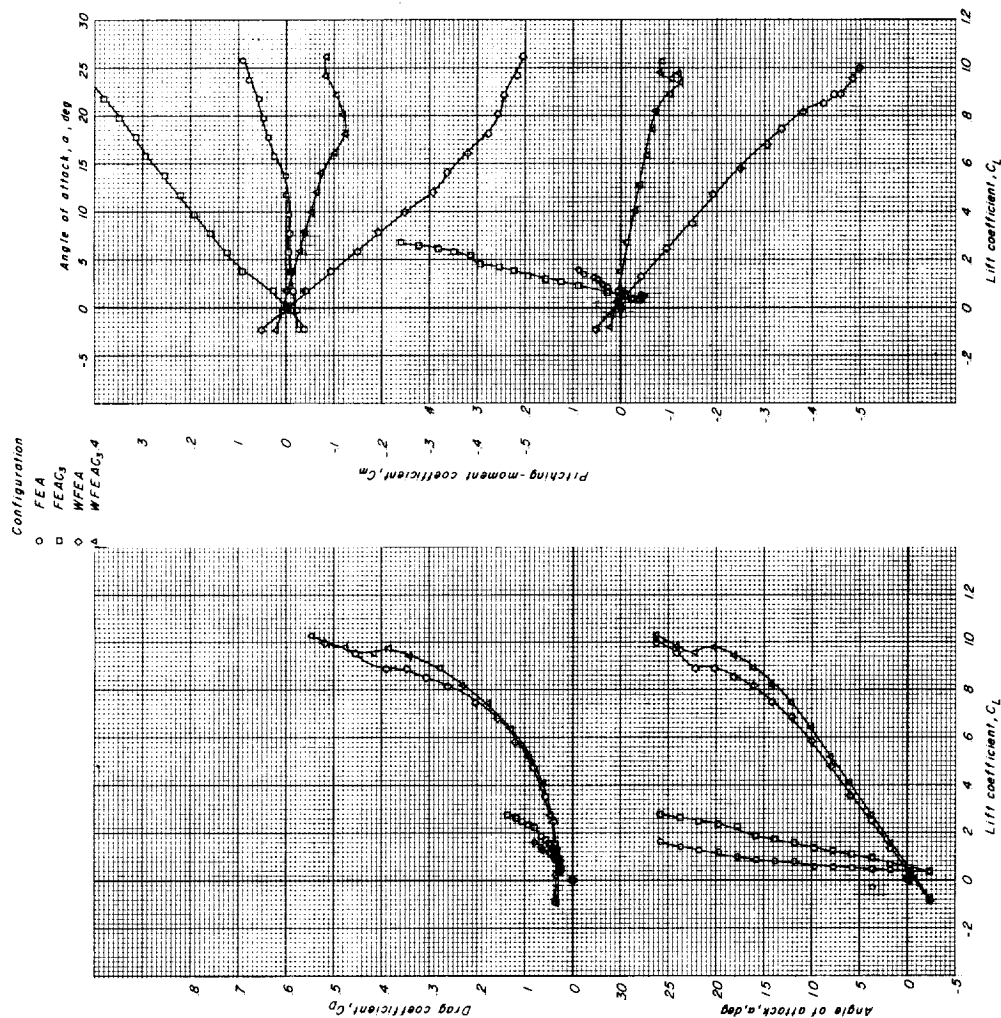
(a) Small canard surface. Moment reference located $0.48\bar{c}_w$ ahead of $\frac{\bar{c}_w}{4}$.

Figure 12.- Aerodynamic characteristics of some of the component parts tested on the fuselage with forebody extended. $\delta_c = 0^\circ$.



(b) Large canard surface. Moment reference located $0.70\bar{c}_w$ ahead of $\frac{\bar{c}_w}{4}$.

Figure 12.- Continued.



(c) Small canard surface in high position. Moment reference located $0.48\bar{c}_w$ ahead of $\frac{\bar{c}_w}{4}$.

Figure 12.- Concluded.

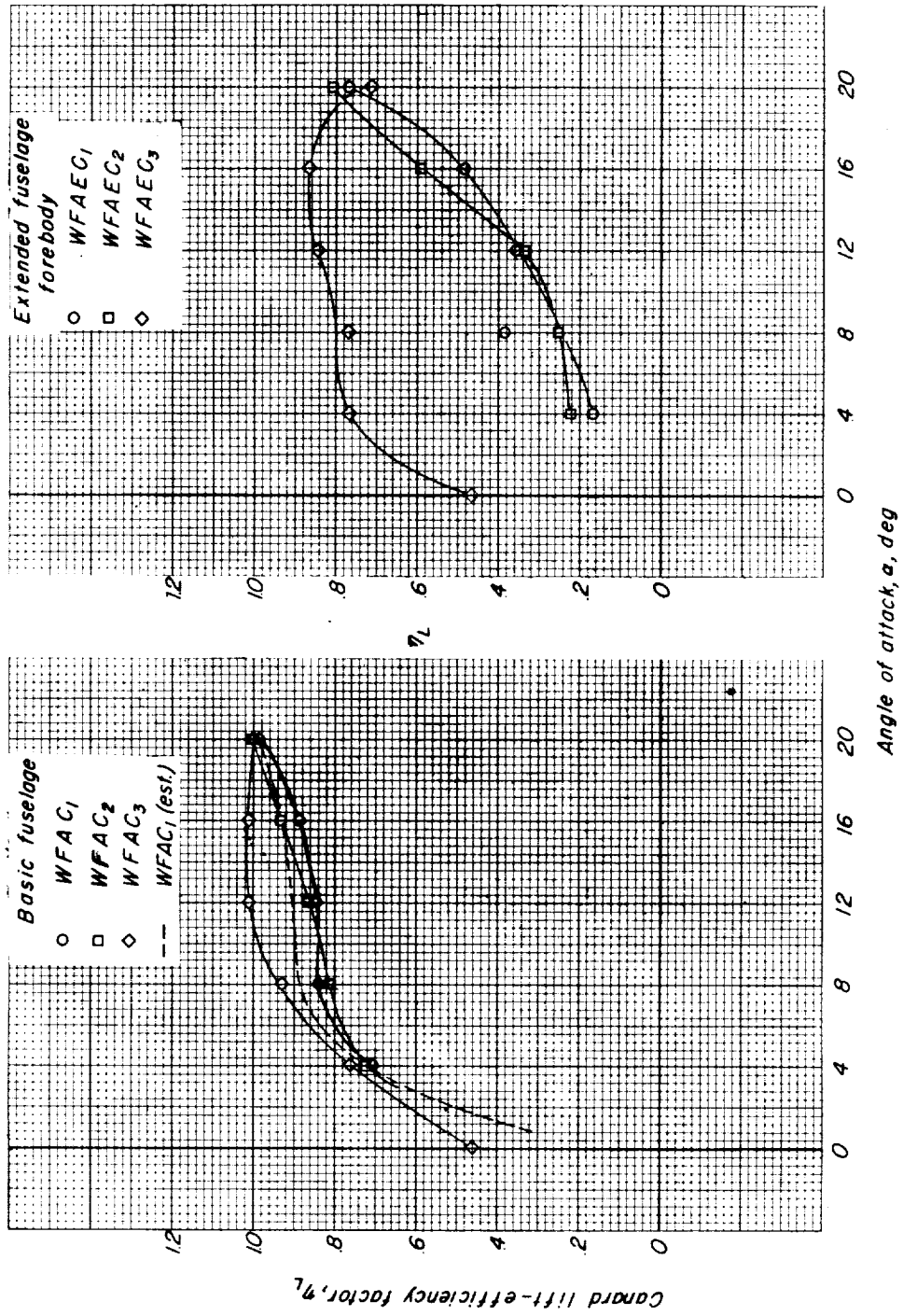


Figure 13.- Trends in canard-surface lift-efficiency factors for various canard-surface arrangements. $\delta_c = 0^\circ$.

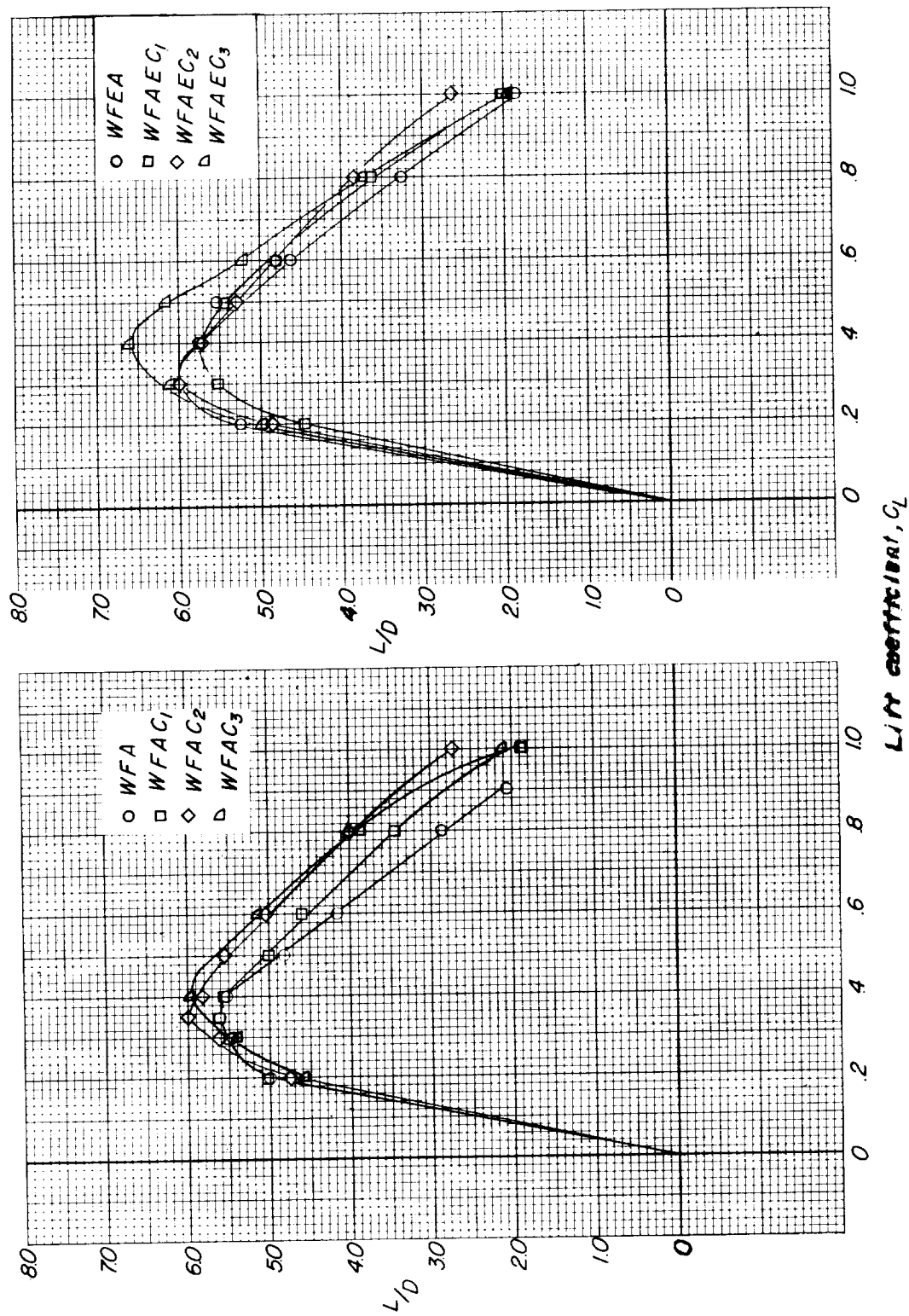


Figure 14.- Trends in untrimmed L/D variations for the various configurations tested.

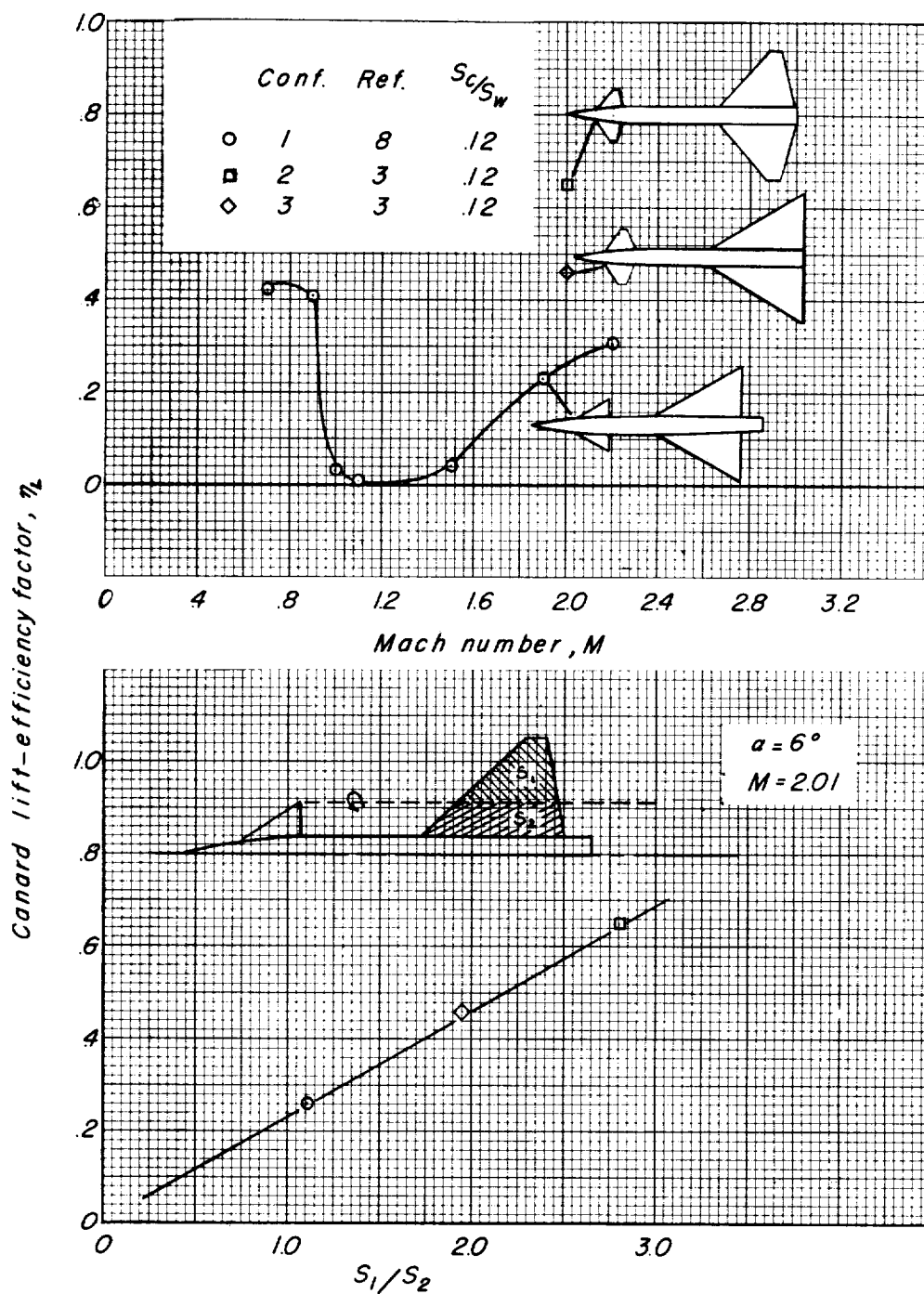


Figure 15.- The effects of configuration and Mach number on canard-surface lift-efficiency factors with canard surface and wing mounted on fuselage center line.

